Figure 6

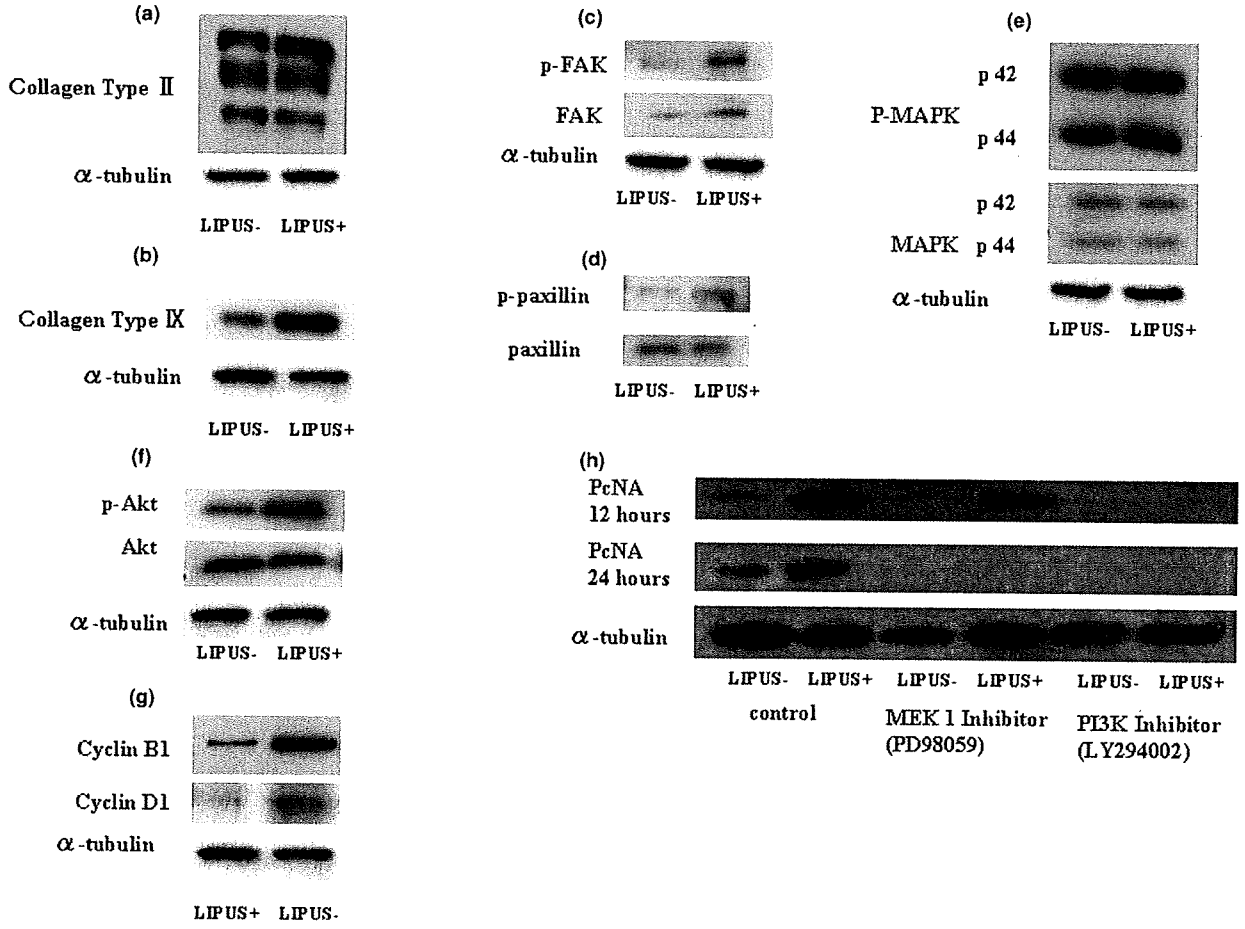

Western blotting analysis. **(a)** Type-II collagen. **(b)** Type-IX collagen. **(c)** Focal adhesion kinase (FAK) and phosphorylated FAK (p-FAK). **(d)** Paxillin and phosphorylated Paxillin (p-Paxillin). **(e)** Mitogen-activated protein kinase (MAPK) and phosphorylated MAPK (p-MAPK). There are no evident differences in the expression levels of total MAPK and p-MAPK between the two groups. **(f)** Akt and phosphorylated Akt (p-Akt). There were no differences found in the intensity the total Akt expression between the two groups, but p-Akt was found at higher levels in the LIPUS group (US+) in comparison with the control group (US-). **(g)** Cyclin B_1 and cyclin D_1. **(h)** Changes of proliferating cell nuclear antigen (PCNA) using MEK1 inhibitor (PD98059) and phosphatidylinositol 3-OH kinase (PI3K) inhibitor (LY294002). Chondrocytes were pretreated with MEK1 inhibitor (PD98059, 250 μM/ml) and PI3K inhibitor (LY294002, 250 μM/ml) for 12 hours and 24 hours followed by stimulation with LIPUS for 20 minutes. Each sample was harvested 2 hours after LIPUS stimulation and the influence of these inhibitors was judged in western blotting analysis of the expression of PCNA.

LIPUS promotes production of collagen type-IX

The immunoblotting analysis in the present study indicated that LIPUS increases the production of collagen type-IX, but not collagen type-II. These results suggest that LIPUS transduces the signals through the intracellular signaling pathway that transactivates the collagen type-IX gene. Although the major constituent of the cartilage matrix is type-II collagen, this matrix also contains collagen types of smaller molecular weights, including type VI, type-IX, type X, type XI, and type XII. These collagens all play regulatory roles in maintaining cartilage. Type-IX collagen is present in zones 1 and 2, and it is said to be involved in promoting chondrocyte proliferation and in the expansion of the cartilage layer [22].

In addition, Eyre and colleagues have earlier reported that type-IX collagen accounts for at least 10% of the collagenous protein in fetal cartilage, but only about 1% to 2% of adult hyaline cartilage – and that the ratio of type-IX collagen to type-II collagen decreases as the cartilage matures [23].

Jarmo and coworkers reported that type-IX collagen has unique cell adhesion properties in comparison with other collagen types, and that it provides a novel mechanism for cell adhesion to the cartilaginous matrix [24]. They demonstrated that the type-IX collagen is a superior cell adhesion protein for chondrocytes. In addition to these reports, Wu and colleagues and Blaschke and colleagues suggested that type-IX collagen may be an important stabilizing factor for cartilage type-II col-

lagen fibrils, since it determines the resistance of the fibrils to swelling in the framework of cartilage [25,26]. Hu and colleagues have also reported that type-IX collagen-deficient mice are prone to developing osteoarthritis [27].

The present results suggest that the chondrocyte proliferation in response to LIPUS is associated with the increase in collagen type-IX expression. Eyre and colleagues reported that the ratio of collagen type-IX to collagen type-II in immature cartilage tissue is greater than that in mature cartilage tissue [23]. The results of the current study support their findings. It is likely that the production of collagen type-IX increases in the current system because of an increase in the number of immature chondrocytes in the cultures. In immature chondrocytes, it was reported that the construction of a peripheral matrix with collagen type-IX also promotes the attachment between the cells and the matrix [26].

Activation of the PI3K/Akt pathway but not the MEK/MAPK pathway by LIPUS

It is very probable that LIPUS transmits signals into the cell via an integrin that acts as a mechanoreceptor on the cell membrane. When ultrasound is transmitted to integrin molecules, this promotes the attachment of various focal adhesion adaptor proteins. Both FAK and Paxillin are in turn phosphorylated as a result of LIPUS exposure initiating this signal transduction.

The integrin/Ras/MAPK/nucleus pathway is considered a general pathway involved in cell proliferation. In the current study, however, MAPK was shown to be similarly activated and phosphorylated regardless of the LIPUS exposure. The results confirmed that MAPK is constitutively activated in both LIPUS-stimulated cells and control cells, probably due to the culture conditions in which the medium is supplemented with 10% FBS. This observation suggests that the significant increase in cell numbers observed in relation to the elevation of type-IX collagen expression is attributable to a signal transduction pathway other than the Ras/MAPK pathway.

The PI3K/Akt pathway, on the other hand, is known to be involved in various functions such as cell survival, proliferation, motility, control of cell size and metabolism [28,29]. In the present experiments, this pathway was found to be newly activated by LIPUS. A previous report also showed that phosphorylated Akt inhibits glycogen synthase kinase-3, which otherwise phosphorylates β-catenin [30]. A high intracellular concentration of β-catenin therefore accumulates when glycogen synthase kinase-3 is inhibited by phosphorylated Akt. In turn, β-catenin translocates to the nucleus and promotes the transcription of its target genes.

The Wnt signaling pathway may also be involved in the increase in the intracellular β-catenin levels [31]. In the current study, LIPUS was found to significantly increase the number of β-catenin-positive cells during enhanced cell proliferation. Both the PI3K/Akt pathway and the Akt/β-catenin pathway are therefore strongly implicated in this process (Figure 7). Moreover, the expression of the cyclin B_1 and cyclin D_1 was found to be elevated in the LIPUS group, providing further evidence that LIPUS promotes the active division of chondrocytes [32,33]. In this regard, Li and colleagues have demonstrated that transforming growth factor beat stimulates cyclin D_1 expression in chondrocytes in part through the activation of β-catenin signaling [34].

Wnt/β-catenin signaling has been reported to play a crucial role in cell proliferation and in the morphogenesis of chondrocytes [35]. Since there is some functional interaction between the PI3K/Akt pathway and Wnt/β-catenin signaling, LIPUS may activate β-catenin signaling via the PI3K/Akt pathway. As indicated in Figure 4c,d, the nuclear localization of β-catenin, as a marker of the β-catenin signaling, was more prominent in LIPUS-stimulated cells than in the control cells, thus indicating this to be the case.

Conclusion

LIPUS promotes type-IX collagen accumulation and enhances the proliferation of cultured chondrocytes. In addition to the general growth factor signaling via the Ras/MAPK pathway, mechanical signal transduction to the nucleus through the integrin/PI3K/Akt pathway is activated by LIPUS, thus resulting in an increased matrix production and proliferation of chondrocytes. Akt seems to control the metabolism of β-catenin via glycogen synthase kinase-3, which phosphorylates β-catenin, and also raises the intracellular β-catenin concentration, which in turn promotes its translocation to the nucleus.

In future studies it will be necessary to elucidate the signals or transcription factors that operate downstream of Akt in this system. Certain membrane receptors or ion channels other than integrins, which may reside upstream of the transcription factors that promote the production of collagen type-IX, should also be investigated.

Competing interests

The authors declare that they have no competing interests.

Authors' contributions

RT performed planning of this study, the *in vitro* experiment, and generalization. AR performed the immunohistochemistry. NK performed western blotting analysis. YM-T was a senior advisor. AF performed cell counting and histological examinations. YT performed western blotting analysis. TS performed ultrasound stimulation. SM was a senior advisor. YY performed histological examinations. KK performed planning and cell culture. IA was a senior advisor. TS was a senior advisor. All authors participated in the conception and design of the study. All authors read and approved the final manuscript.

Figure 7

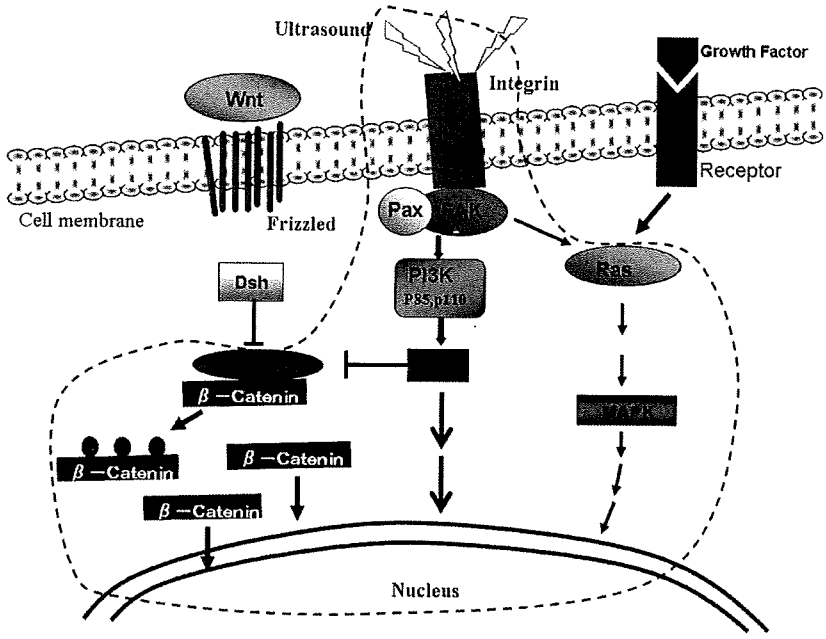

Signal transduction pathways activated by low-intensity pulsed ultrasound. Area enclosed with a black broken line is the signaling pathway specified in the present experiment. One of the receptors of low-intensity pulsed ultrasound (LIPUS) is through integrin, and the integrin/mitogen-activated protein kinase (MAPK) pathway is activated to the same extent in both the LIPUS group and the control group. The integrin/phosphatidylinositol 3 kinase (PI3K)/Akt pathway, however, was further activated by LIPUS. The expression of β-catenin, which is downstream of the Akt signaling pathways, is also increased by LIPUS. FAK, focal adhesion kinase; GSK-3, glycogen synthase kinase-3; Pax, Paxillin.

Acknowledgements

The authors thank Ms Kumiko Tanaka for her valuable technical assistance. The present study was supported by Grants-in-Aid for Scientific Research (No. 0517591586, 2005–2006) from the Japanese Ministry of Education, Culture, Sports, Science and Technology, and Grants of the Kenkyu-Senryaku Project (2007) from Yokoham City University.

References

1. Iwata H: **Phamacologic and clinical aspects of intraarticular injection of hyaluronate.** *Clin Orthop* 1993, **289**:285-291.
2. Alarid ET, Schlechter NL, Russell SM, Nicoll CS: **Evidence suggesting that insulin-like growth factor-I is necessary for the trophic effects of insulin on cartilage growth *in vivo*.** *Endocrinology* 1992, **130**:2305-2309.
3. Schlechter NL, Russell SM, Spencer EM, Nicoll CS: **Evidence suggesting that the direct growth-promoting effect of growth hormone on cartilage *in vivo* is mediated by local production of somatomedin.** *Proc Natl Acad Sci USA* 1986, **83**:7932-7934.
4. Salter MD, Millward-Sadler JS, Nuki G, Wright OM: **Integrin–interleukin-4 mechanotransduction pathways in human chondrocytes.** *Clin Orthop* 2001, **391S**:49-60.
5. Sah RL, Kim YJ, Doong JY, Grodzinsky AJ, Plaas AH, Sandy JD: **Biosynthetic response of cartilage explants to dynamic compression.** *J Orthop Res* 1989, **7**:619-636.
6. Sah RL, Trippel SB, Grodzinsky AJ: **Differential effects of serum, IGF-I, and FGF-2 on the maintenance of cartilage physical properties during long-term culture.** *J Orthop Res* 1996, **14**:44-52.
7. Hangody L, Kish G, Kárpáti Z, Szerb I, Udvarhelyi I: **Arthroscopic autogenous osteochondral mosaicplasty for the treatment of femoral condylar articular defects. A preliminary report.** *Knee Surg Sports Traumatol Arthrosc* 1997, **5**:262-267.
8. Ochi M, Uchio Y, Tobita M, Kuriwaka M: **Current concepts in tissue engineering technique for repair of cartilage defect.** *Artif Organs* 2001, **25**:172-179.
9. Ochi M, Uchio Y, Matsusaki M, Wakitani S, Sumen Y: **Cartilage repair – a new surgical procedure of cultured chondrocyte transplantation.** In *Controversies in Orthopaedic Sports Medicine* Edited by: Chan KM, FU F. Philadelphia, PA: Lippincott-Ravin; 1998:549-563.
10. Mizuno S, Tateishi T, Ushida T, Glowacki J: **Hydrostatic fluid pressure enhances matrix synthesis and accumulation by bovine chondrocytes in 3-D culture.** *J Cell Physiol* 2002, **193**:319-327.
11. Wright M, Jobanputra P, Bavington C, Salter DM, Nuki G: **Effects of intermittent pressure-induced strain on the electrophysiology of cultured human chondrocytes: evidence for the presence of stretch-activated membrane ion channels.** *Clin Sci* 1996, **90**:61-71.
12. Takeuchi R, Saito T, Ishikawa H, Takigami H, Dezawa M, Ide C, Itokazu Y, Ikeda M, Shiraishi T, Morishita S: **Effects of vibration and hyaluronic acid on activation of 3-D cultured chondrocytes.** *Arthritis Rheum* 2006, **54**:1897-1905.
13. Nishikori T, Ochi M, Uchio Y, Maniwa S, Kataoka H, Kawasaki K, Katsube K, Kuriwaka M: **Effects of low-intensity pulsed ultrasound on proliferation and chondroitin sulfate synthesis of cultured chondrocytes embedded in Atelocollagen gel.** *J Biomed Mater Res* 2002, **59**:201-206.
14. Parvizi J, Parpura V, Greenleaf JF, Bolander ME: **Calcium signaling is required for ultrasound-stimulated aggrecan synthesis by rat chondrocytes.** *J Orthop Res* 2002, **20**:51-57.
15. Zhang ZJ, Huckle J, Francomano CA, Spencer RG: **The effects of pulsed low intensity ultrasound on chondrocyte viability, proliferation, gene expression and matrix production.** *Ultrasound Med Biol* 2002, **29**:1645-1651.
16. Huang MH, Ding HJ, Chai CY, Huang YF, Yang RC: **Effects of sonication on articular cartilage in experimental osteoarthritis.** *J Rheumatol* 1997, **24**:1978-1984.
17. Tang CH, Yang RS, Huang TH, Lu DY, Chuang WJ, Huang TF, Fu WM: **Ultrasound stimulates cyclooxygenase-2 expression and increase bone formation through integrin, focal adhesion**

kinase, phosphatidylinositol 3-kinase, and Akt pathway in osteoblast. *Mol Pharmacol* 2006, **69:**2047-2057.
18. Kronenberg MH: **Developmental regulation of the growth plate.** *Nature* 2003, **423:**332-336.
19. Itoh H, Aso Y, Furuse M, Noishiki Y, Miyata T: **A honeycomb collagen carrier for cell culture as a tissue engineering scaffold.** *Artif Organs* 2001, **25:**213-217.
20. Nawa G, Ueda T, Mori S, Yoshikawa H, Fukuda H, Ishiguro S, Funai H, Uchida A: **Prognostic significance of Ki 67 (MIB1) proliferation index and p53 over-expression in chondrosarcomas.** *Int J Cancer* 1996, **69:**86-91.
21. Cook DS, Salkeld SL, Popich-Parton LS, Ryaby JP, Jones DG, Barrack RL: **Improved cartilage repair after treatment with low-intensity pulsed ultrasound.** *Clin Orthop* 2001, **391S:**231-243.
22. Cay MK, Alvin PLK, David FH, Holmes SLS, Michael EG: **Type X collagen, a product of hypertrophic chondrocytes.** *Biochem J* 1985, **27:**545-554.
23. Eyre DR, Apon S, Wu JJ, Ericsson LH, Walsh KA: **Collagen type IX: evidence for covalent linkages to type II collagen in cartilage.** *FEBS Lett* 1987, **17:**237-241.
24. Jarmo K, Juha J, Mira T, Joni Y, Liosa N, Tiina V, Piia V, Varpu M, Petri N: **The fibril-associated collagen IX provides a novel mechanism for cell adhesion to cartilaginous matrix.** *J Biol Chem* 2004, **279:**51677-51687.
25. Wu JJ, Woods PE, Eyre DR: **Identification of cross-linking sites in bovine cartilage type IX collagen reveals an antiparallel type II – type-IX molecular relationship and type IX to type IX bonding.** *J Biol Chem* 1992, **267:**23007-23014.
26. Blaschke UK, Eikenberry EF, Hulmes DJS, Galla HJ, Bruckner P: **Collagen IX nucleates self-assembly and limits lateral growth of cartilage fibrils.** *J Biol Chem* 2000, **275:**10370-10378.
27. Hu K, Xu L, Cao L, Flahiff M, Brussiau J, Ho K, Setton A, Youn I, Guilak F, Olsen BR, Li Y: **Pathogenesis of osteoarthritis-like changes in the joints of mice deficient in type IX collagen.** *Arthritis Rheum* 2006, **54:**2891-2900.
28. Downward J: **PI(3)Kinase, Akt and cell survival.** *Semin Cell Dev Biol* 2004, **15:**177-182.
29. Gustin AJ, Korgaonkar KC, Pincheira R, Li Q, Donner BD: **Akt regulates basal and induced processing NF-kB2 (p100) to p 52.** *J Biol Chem* 2006, **281:**16473-16481.
30. Darren AEC, Dario RA, Philip C, Mirjana A, Brian AH: **Inhibition of glycogen synthase kinase-3 by insulin mediated by protein kinase B.** *Nature* 1995, **378:**785-789.
31. Shtutman M, Zhurinsky J, Simcha I, Albanese C, Pestell MR, Ben-Ze' A: **The cyclin D_1 gene is a target of the β-catenin/LEF-1 pathway.** *Cell Biol* 1999, **96:**5522-5527.
32. Hwang A, McKenna WG, Muschel RJ: **Cell cycle-dependent usage of transcriptional start sites. A novel mechanism for regulation of cyclin B1.** *J Biol Chem* 1998, **273:**31505-31509.
33. Sgerr CJ: **Cancer cell cycles.** *Science* 1996, **274:**1672-1677.
34. Li TF, Chen D, Wu Q, Chen M, Sheu TJ, Schwarz EM, Drissi H, Zuscik M, O'Keefe RJ: **Transforming growth factor-β stimulates cyclin D_1 expression through activation of β-catenin signaling in chondrocytes.** *J Biol Chem* 2006, **281:**21296-21304.
35. Yano F, Kugimiya F, Ohba S, Ikeda T, Chikuda H, Ogasawara T, Ogata N, Takato T, Nakamura K, Kawaguchi H, Chung U: **The canonical Wnt signaling pathway promotes chondrocyte differentiation in a Sox9-dependent manner.** *Biochem Biophys Res Commun* 2005, **333:**1300-1308.

FEBS Letters 582 (2008) 1795–1801

The wheat germ cell-free based screening of protein substrates of calcium/calmodulin-dependent protein kinase II delta

Takashi Masaoka[a], Mayuko Nishi[c], Akihide Ryo[c], Yaeta Endo[a,b,d,*], Tatsuya Sawasaki[a,b,d,*]

[a] *Cell-free Science and Technology Research Center, Ehime University, Matsuyama 790-8577, Japan*
[b] *The Venture Business Laboratory, Ehime University, Matsuyama 790-8577, Japan*
[c] *AIDS Research Center, National Institute of Infectious Diseases, 1-23-1 Toyama, Shinjuku-ku, Tokyo 162-8640, Japan*
[d] *RIKEN Genomic Sciences Center, 1-7-22 Suehiro-cho, Tsurumi, Yokohama 230-0045, Japan*

Received 22 February 2008; revised 19 March 2008; accepted 2 April 2008

Available online 16 May 2008

Edited by Jesus Avila

Abstract Calcium/calmodulin-dependent protein kinase II (CaMKII) plays a crucial role in mediating calcium signaling. Here, we demonstrate a method for screening substrates phosphorylated by human CaMKIIδ using a wheat cell-free system. The cell-free mixture expressing CaMKIIδ was incubated with HeLa extracts and radiolabeled ATP. From analysis of two-dimensional electrophoresis gels and mass spectrometry, two proteins were found. The cell-free based in vitro kinase assay revealed that CaMKIIδ phosphorylates eukaryotic translation initiation factor 4B and stress-induced phosphoprotein 1 (STIP1), the latter on Ser189. Furthermore, constitutively-active CaMKIIδ phosphorylated STIP1 in HeLa cells and dramatically promoted nuclear localization of STIP1, suggesting that calcium signals via CaMKIIδ may regulate subcellular localization of STIP1. This approach may be a useful tool for target screening of protein kinases.

Structured summary:
MINT-6538664: *CAMK2D* (uniprotkb:Q13557) *phosphorylates* (MI:0217) *STIP1* (uniprotkb:P31948) by *protein kinase assay* (MI:0424)
MINT-6538652: *CAMK2D* (uniprotkb:Q13557) *phosphorylates* (MI:0217) *EIF4B* (uniprotkb:P23588) by *protein kinase assay* (MI:0424)

*Keywords*Cell-free protein synthesis; Protein kinase; Phosphorylation; Substrate screening; Calcium/calmodulin-dependent protein kinase II; Stress-induced phosphoprotein 1

1. Introduction

Calcium, Ca^{2+}, is one of the most important signals in eukaryotic cells and induces many biochemical protein functions [1]. Multifunctional Ca^{2+}/calmodulin-dependent protein kinase II (CaMKII) is a major mediator of Ca^{2+} signaling that translates elevation of intracellular Ca^{2+} level into phosphorylation of target proteins that participate in a wide range of cellular functions including fertilization, proliferation, differentiation, learning and memory. Four isoforms (α, β, γ and δ) of CaMKII are found in mammalian genomes [2]. The γ and δ isoforms are ubiquitously expressed in most tissues, whereas the α and β isoforms are found abundantly in brain. The identification of substrate proteins of CaMKII would be useful in understanding molecular regulatory mechanisms by Ca^{2+} and phosphorylation signaling.

One of the simple biochemical approaches to identifying kinase substrates is to incubate protein kinase with cell extracts, and then to analyze the phosphorylated proteins by two-dimensional electrophoresis (2-DE) [3]. The advantage of this method is that it can screen thousands of natural substrates in the cell. However, it is often difficult to prepare sufficient functionally active kinases for the biochemical analysis because conventional recombinant protein production technologies, as represented by *Escherichia coli* cells, cannot produce those proteins that affect the physiology of the host cell. In addition, the cell-based protein production systems require the high quality purification of protein kinase for the screening because they have high phosphorylation activities of endogenous protein kinases. However, the quality control is one of the most time-consuming steps. We developed a wheat germ cell-free protein production system [4–7], and recently have successfully produced over ~400 eukaryotic protein kinases [8,9]. Furthermore, the wheat cell-free system had very low activities of endogenous protein kinases [10]. Taking advantage of this feature, we attempted to identify substrates of CaMKIIδ (CaMKIId) in HeLa cells by mixing of the HeLa cell extracts and the wheat cell-free extracts expressing CaMKIId. Two phosphorylated proteins were identified by matrix-assisted laser desorption/ionization time-of-flight mass spectrometry (MALDI-TOF-MS) after separation on 2-DE gel. Confirmation of protein phosphorylations and identification of phosphorylation site were investigated by an in vitro kinase assay based on the cell-free system. The biological significance of the phosphorylation site was substantiated by cotransfection analysis. From these studies, we have

*Corresponding authors. Address: Cell-free Science and Technology Research Center, Ehime University, Matsuyama 790-8577, Japan. Fax: +81 89 927 9941.
E-mail addresses: yendo@eng.ehime-u.ac.jp (Y. Endo), sawasaki@eng.ehime-u.ac.jp (T. Sawasaki).

Abbreviations: CaMKIId, calcium/calmodulin-dependent protein kinase II delta; DHFR, dihydrofolate reductase; 2-DE, two-dimensional gel electrophoresis; MALDI-TOF-MS, matrix-assisted laser desorption/ ionization time-of-flight mass spectrometry; bls, biotin ligation site; STIP1, stress-induced phosphoprotein 1; eIF4B, eukaryotic translation initiation factor 4B; mST11, murine stress-inducible protein 1; CA, constitutively active; KD, kinase dead

0014-5793/$34.00
doi:10.1016/j.febslet.2008.04.060

successfully identified stress-induced phosphoprotein 1 (STIP1) and eukaryotic translation initiation factor 4B (eIF4B) as novel substrates of CaMKIId, and also could present a simple way to identify substrates of protein kinase using the crude kinase expressed in the cell-free system.

2. Materials and methods

2.1. General

Details of the following procedures have been either described or cited previously [4–9]: generation of DNA template by PCR using split-primers, synthesis of mRNA, protein synthesis in parallel, estimation of amount of protein synthesized by means of densitometric scanning of the Coomassie brilliant blue® (CBB)-stained band and autoradiography. The wheat germ extract was purchased from CellFree Sciences Co. (Yokohama, Japan).

2.2. Plasmid construction

Three genes, CaMKIId (GenBank accession number AF071569), STIP1 (gi:5803180) and eIF4B (gi:18146613) were amplified from commercially available human cDNA (biochain, Hayward, CA) or cDNAs from HeLa cells by PCR with LA Taq polymerase (TakaraBIO, Otsu, Shiga) and primers (5′-GAGACTCGAGATGGCTTCGACCACC-ACCTG and 5′-GAGAGGATCCTCAGATGTTTTGCCACAAAG for CaMKIId, 5′-CCACCCACCACCACCAATGGAGCAGGTC-AATGAG and 5′-TCACCGAATTGCAATCAG for STIP1, 5′-CCACCCACCACCACCAATGGCGGCCTCAGCAAAAAAG and 5′-CTATTCGGCATAATCTTCTCCC for eIF4B,), and then inserted into pT7blue vector (Merck). FLAG-STIP1 was amplified by PCR and cloned into pcDNA3.1(−)(Invitrogen). The point mutants of eIF4B (S93A, S422A, S425A, S498A, S504A, S597A), STIP1 (S189A, T198A), constitutively active (CA) CaMKIId (T287D) and kinase dead (KD) CaMKIId (T287D, K43M) were generated by PCR mutagenesis using the Quikchange mutagenesis method (Stratagene, La Jolla, CA).

2.3. Construction of transcriptional template and in vitro transcription

Construction of CaMKIId transcriptional template by split-primer PCR and in vitro transcription were performed as described [7]. Transcriptional templates of STIP1, eIF4B and their mutants were constructed in fusion forms containing a biotin ligation site (bls) at the N-terminus (that is essential for protein biotinylation) [10] using the split primer PCR method with E01-bls-S1 (5′-GGTGACACTATA-GAACTCACCTATCTCTCTACACAAAACATTTCCCTACATAC-AACTTTCAACTTCCTATTATGGGCCTGAACGACATCTTCG-AGGCCCAGAAGATCGAGTGGCACGAACTCCACCCACCAC-CACCAATG) primer instead of primer-2.

2.4. Wheat germ cell-free protein production

Proteins were synthesized in a dialysis cup (molecular weight cutoff 12000; Biotech International) overnight using published protocols [7]. SDS–PAGE with CBB staining was used to determine target protein yields ('total', 'soluble' and 'pellet' fractions). Synthesized CaMKIId was exchanged into phosphoreaction buffer (50 mM Tris–HCl, pH 7.5, 10 mM $MgCl_2$, 0.5 mM DTT) using G-25 spin columns (Amersham). In vitro transcription and cell-free protein synthesis based on bilayer reaction mode were performed as described [6]. The biotinylated proteins were obtained as described previously [10].

2.5. Screening of CaMKIId substrate and 2-DE

HeLa cells ($\sim 1 \times 10^7$) were harvested by centrifugation and suspended in 100 μl of extraction buffer (50 mM Tris–HCl, pH 7.5, 1 mM EDTA, 6 mM beta-mercaptoethanol). The mixture was lysed using the freeze–thaw method. After centrifugation for 15 min at $20000 \times g$ the supernatant was exchanged into phosphoreaction buffer using a G-25 spin column. HeLa cell extracts (20 μl) were pre-incubated in 7 μl of crude CaMKIId (or dihydrofolate reductase (DHFR) as a control), 100 μM ATP, 7 μl of 5× activation buffer (containing 5 mM $CaCl_2$, 5 μM calmodulin from human brain (ALEXIS corporation, Lausen, Switzerland), 0.1 mg/ml BSA) and 2 μl of 5× phosphoreaction buffer at 30 °C for 20 min. 370 kBq of [γ-^{32}P] ATP (*ICN*) was then added to the reaction mixture (35 μl of total volume) and incubated at 30 °C for 30 min. Following the reaction, proteins were separated on 2-DE gel. First-dimension isoelectric focusing was performed using pH 3–10 immobilized pH gradient (IPG) strips (Bio-Rad). IPG strips were rehydrated in rehydration buffer (9.8 M Urea, 0.5% CHAPS, 10 mM DTT) and reaction mixtures were focused at 4000 V and 25 μ A_{max}/gel for 30000 V h. After isoelectric focusing, IPG strips were washed for 5 min with equilibration buffer (6 M Urea, 2% SDS, 0.375 M Tris–HCl, pH 8.8, 20% glycerol, 130 mM DTT) four times and then IPG strips were applied to the second-dimension 12.5% SDS–PAGE. Finally, we determined which proteins were phosphorylated by gel image analysis of CBB staining and autoradiograms by BAS-2500 (FUJIFILM, Tokyo, Japan).

2.6. Identification of phosphorylated protein by MALDI-TOF-MS

After 2-DE gel image analysis, two protein spots were selected, and analyzed by peptide mass fingerprinting using MALDI-TOF-MS and database searching (MS-Fit). The peptide mass fingerprinting was performed by Promega Corporation.

2.7. In vitro phosphorylation assay

To obtain purified CaMKIId of wildtype, CA or KD form, GST-TEVsite-CaMKIId fused genes were inserted into pEU3b vector [7] and were used for the cell-free system as described above. The GST-fusion proteins were purified on Glutathione Sepharose 4B (Amersham), and then the CaMKIId proteins were recovered by on-column cleavage using AcTEV protease (Invitrogen) which cleaves at the TEVsite.

Cell-free synthesized bls-STIP1 and bls-eIF4B were biotinylated by the cell-free BirA system [10], and 20 μl of each biotinylated protein coupled to 10 μl of MagneSphere Strept beads (Promega) and incubated at 26 °C for 1 h. After incubation, protein-coupled beads were washed three times with phosphoreaction buffer and then incubated the beads with 200 ng of purified recombinant CaMKIId, 3 μl of 5× activation buffer, 3 μl of 5× phosphoreaction buffer and 37 kBq of [γ-^{32}P]ATP in a total volume of 15 μl at 30 °C for 20 min. After reaction, the beads were washed three times with 1× PBS(−), then boiled in sample buffer (50 mM Tris–HCl, pH 6.8, 2% SDS, 1% 2-mercaptoethanol, 0.004% bromophenol blue) and separated by 12% polyacrylamide gels. Phosphorylation was visualized by autoradiography.

2.8. Cell culture, transient transfections

HeLa cells were cultured in Dulbecco's modified Eagle's medium supplemented with 10% fetal bovine serum and 1% penicillin (100 mg/ml)/streptomycin (50 μg/ml). Transient transfections were carried out using Effectene Transfection Reagent (QIAGEN). Twenty-four hours after transfection, the cells were lysed and subjected to SDS–PAGE. Mobility shift detection of phosphorylated proteins was performed using phos-tag acyrylamide gel (Nard Institute Inc., Amagasaki, Japan) according to the manufacture's instruction and then analyzed by immunoblotting with anti-FLAG M2 antibodies (SIGMA).

2.9. Fluorescence imaging

HeLa cells on coverslips were transfected with FLAG-STIP1 and co-transfected with empty vector (EV), CA or KD mutants of CaMKIId using Effectene Transfection Reagent (QIAGEN), according to the manufacturer's instructions. Twenty-four hours after transfection, the cells were fixed with 3% formaldehyde and washed with PBS, and were immunostained with anti-FLAG M2 antibody (SIGMA) and then 4′,6-diamidino-2-phenylindole (DAPI). After washing with PBS, slides were visualized under a fluorescent microscope (Olympus, Tokyo, Japan) as described previously [11].

3. Results

3.1. Cell-free protein synthesis of CaMKIId and measurement of product quality

In order to assess the quality of the cell-free synthesized protein, we measured the amount, solubility and phosphorylating activity of CaMKIId. The amount and solubility of the CaMKIId as estimated from densitometric scanning of the bands

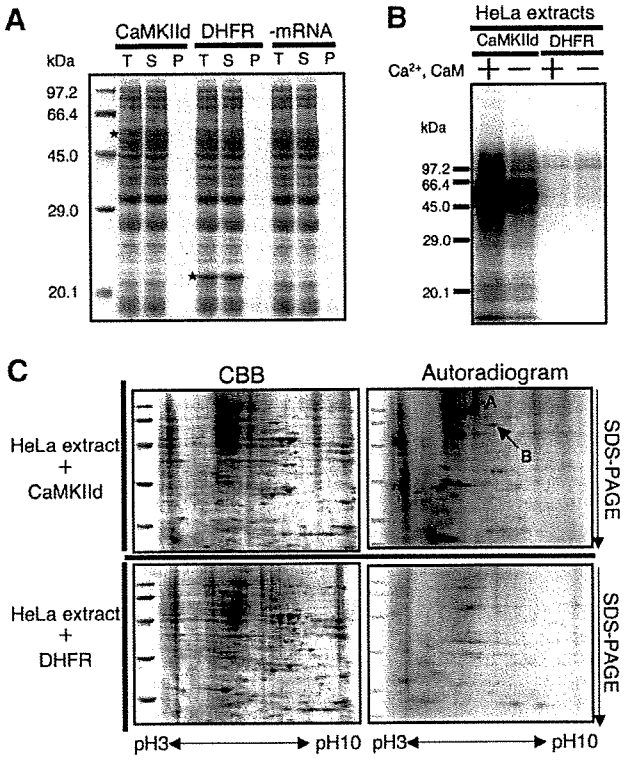

Fig. 1. Production and solubility of cell-free synthesized CaMKIId and autoradiograms of CaMKIId reactions. (A) Cell-free translation products were separated by SDS–PAGE and stained with CBB. T, S and P, respectively, mark total translation product, the supernatant fraction after centrifugation at 30000 × *g* for 15 min and precipitate. Asterisks mark the synthesized proteins. (B) HeLa cell extracts were incubated with CaMKIId, Ca^{2+} and calmodulin at 30 °C for 20 min in the presence of [γ-^{32}P]ATP, then the reaction mixture separated by SDS–PAGE. (C) Reaction mixtures were separated by 2-DE gel and the phosphorylated proteins detected by autoradiography to determine the candidate CaMKIId substrates.

were ~200 μg/ml and ~90%, respectively (Fig. 1A). We investigated whether the wheat cell-free extract expressing CaMKIId (crude CaMKIId) could phosphorylate proteins in the HeLa cell extracts with or without Ca^{2+}/calmodulin in the presence of radiolabeled ATP. The phosphorylation was detected by autoradiography after SDS–PAGE. Protein phosphorylation in HeLa cell extracts was dramatically induced by addition of CaMKIId and Ca^{2+}/calmodulin (Fig. 1B). These results indicate that the wheat cell-free system could synthesize the CaMKIId in a folded state and that phosphorylating activity is strongly enhanced by supplementing with Ca^{2+}/calmodulin without a purification step. Interestingly four protein bands of ~90 kDa, ~64 kDa, ~50 kDa and 43 kDa were strongly phosphorylated by CaMKIId. The phosphorylating activity of CaMKIId in the absence of both Ca^{2+} and calmodulin indicates that there is partial activation by Ca^{2+}/calmodulin from HeLa cells and/or wheat germ extracts. In contrast, the addition of the wheat extract expressing DHFR (crude DHFR), as a control, had no significant influence on protein phosphorylation even in the presence of Ca^{2+}/calmodulin, indicating that the endogenous kinase activity in the wheat extract is low, and the wheat germ cell-free system is suitable for screening of substrate proteins phosphorylated by CaMKIId.

3.2. Identification of CaMKIId substrate proteins

The substrate screening was conducted by mixing crude CaMKIId with HeLa cell extracts and [γ-^{32}P] ATP followed by 2-DE gel. The total protein spots and the phosphorylated spots by CaMKIId were analyzed by gel images of CBB staining and autoradiogram, respectively (Fig. 1C). By the analysis, more than 90 phosphorylated spots were observed. Of these, 32 proteins were CaMKIId-dependently phosphorylated and 11 of them were detectable by CBB staining. Six of the 11 were derived from HeLa cell extracts. From separation quality of the CBB-staining spots, two HeLa proteins (marked in Fig. 1C) strongly phosphorylated were selected as candidate substrates and then were used for peptide mass fingerprinting by MALDI-TOF-MS. The data from each spot were submitted to MS-Fit. Seventeen and 11 of the 30 submitted ions were matched to theoretical tryptic peptides from eIF4B and STIP1, respectively (Fig. 2). The molecular weight of STIP1 and eIF4B were calculated as 62.6 and 69.1 kDa, respectively. These corresponded to the size of each spot on the 2D-gel. Although in vitro phosphorylation of STIP1 and eIF4B by some protein kinases has been reported [12–14], the two proteins are new candidate substrates of CaMKIId.

3.3. Confirmation of STIP1 and eIF4B phosphorylation

In the next step, an in vitro kinase assay was used to examine whether CaMKIId directly phosphorylates the two proteins. For this, STIP1 and eIF4B genes were cloned from cDNAs prepared from total RNA of HeLa cells, and were fused with bls at its N-terminus by split-primer PCR (see Section 2) for simple purification. After cell-free protein production, each product was biotinylated, and was purified by using streptavidin-conjugated magnetic beads. In vitro kinase assays were performed by which the purified CaMKIId and substrate proteins were incubated with radiolabeled ATP, and then confirmed direct phosphorylation of STIP1 and eIF4B by CaMKIId (Fig. 3A). The molecular weight of STIP1 and eIF4B, calculated as 62.6 and 69.1 kDa, respectively, were corresponded to the size of each spot on the 2D-gel. These data show that STIP1 and eIF4B are new in vitro substrates for CaMKIId.

3.4. Mutational analysis of STIP1 for identification of the site phosphorylated by CaMKIId

Although there is little known about the biological effect of phosphorylation of eIF4B, it is suggested that phosphorylation of Ser422 by p70S6K interferes with translation initiation in vivo[15]. A phosphorylation site in human STIP1 has been reported to be Y354 [16], but it is not known about Ser/Thr residues. However, phosphorylation on Ser189 and Thr198 has been found in its mouse homolog, murine stress-inducible protein 1 (mSTI1), and has been suggested that these two phosphorylations control nuclear transport [12]. To further understand the functions of CaMKIId with respect to the substrate proteins, we performed mutational analysis to identify the phosphorylation site(s) of STIP1 and eIF4B by CaMKIId. The Ser or Thr residues known as phosphorylation sites in STIP1 and eIF4B were mutated to alanine, and then the point mutants were used for the in vitro kinase assay. There was no effect on the phosphorylation of six eIF4B mutants (S93A, S422A, S425A, S498A, S504A, S597A, data not shown). However, the mutational analysis of STIP1 showed that Ser189 was

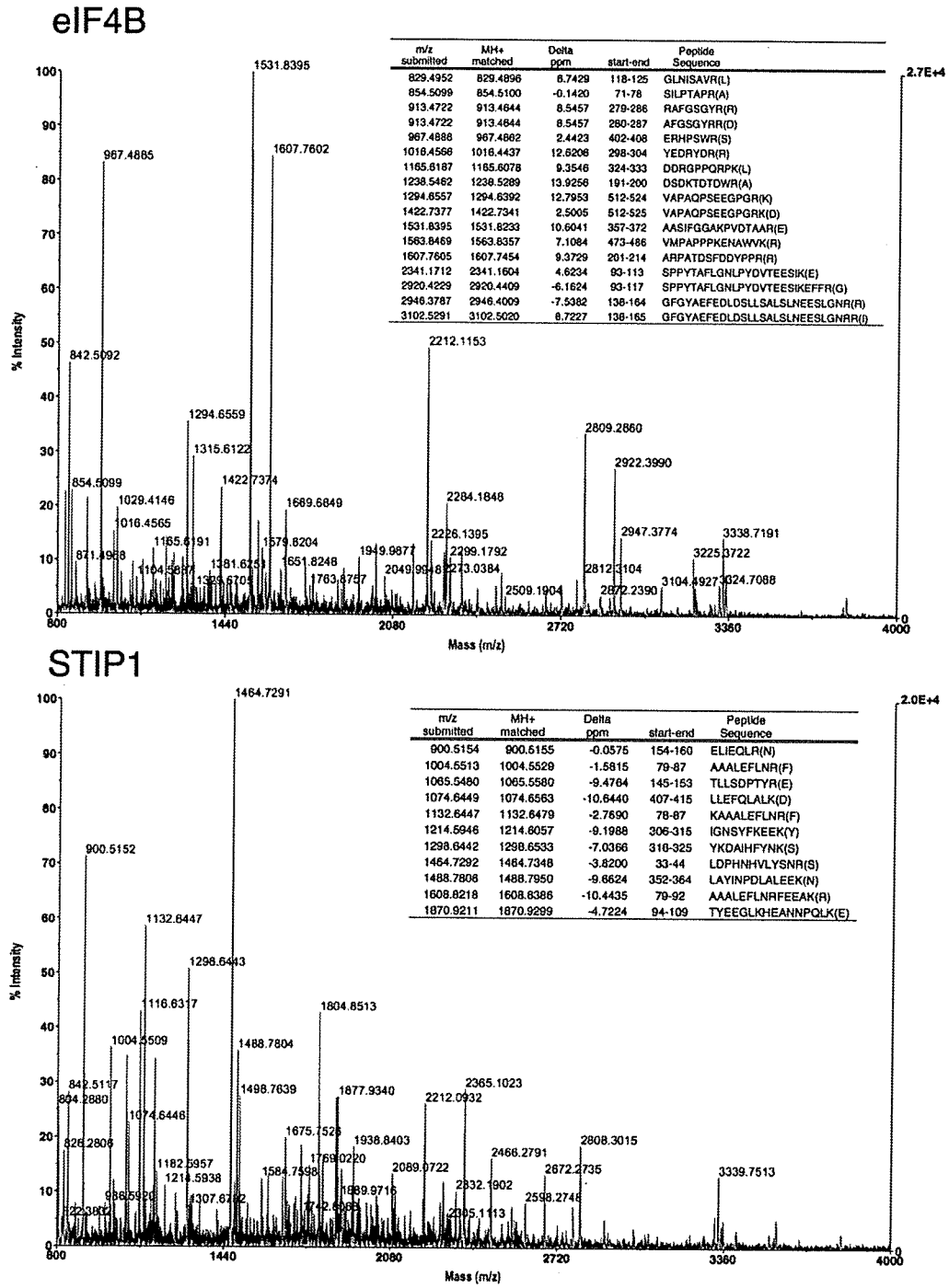

Fig. 2. MALDI-TOF-MS spectra of tryptic digests of candidate substrates. Two candidate substrate spots (A and B; indicated by arrows in Fig. 1C) were excised from 2-DE gel and were digested with trypsine. The resulting peptides were analyzed using MALDI-TOF-MS. The two candidate CaMKIId substrates were identified as STIP1 and eIF4B from the MS-Fit results.

the target residue of CaMKIId phosphorylation and T198A mutant was phosphorylated by CaMKIId (Fig. 3B).

3.5. *In vivo phosphorylation of STIP1 by CaMKIId promotes nuclear translocation*

To examine the in vivo phosphorylation of STIP1 by CaMKIId, we constructed constitutively active (CA) or kinase dead (KD) mutants of CaMKIId. The in vitro phosphorylation of STIP1 by purified CA or KD mutants showed that CA mutant phosphorylated STIP1 even in the absence of Ca^{2+}/calmodulin, whereas KD mutant had no kinase activity (Fig. 4A). We utilized the phos-tag gel system to monitor the in vivo protein phosphorylation as shifted bands [17]. HeLa cells were transfected with FLAG-STIP1 and co-transfected with empty

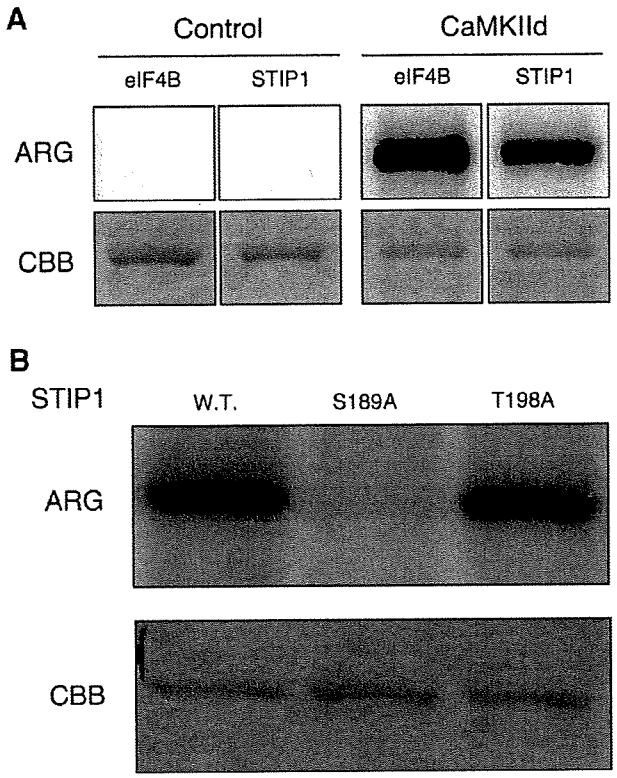

Fig. 3. In vitro kinase assay with STIP1 and eIF4B and identification of phosphorylation site on STIP1. (A) The STIP1 and eIF4B genes were cloned from HeLa cDNAs and the gene products synthesized as bls fused protein using the cell-free system. The two biotinylated proteins were purified using streptavidin-conjugated magnetic beads, then the beads were suspended in reaction mixture containing CaMKIId (or DHFR as a control), [γ-^{32}P]ATP, Ca^{2+} and calmodulin and incubated at 30 °C for 30 min. After washing, proteins were separated by 12.5% SDS–PAGE and results were visualized by autoradiography. (B) Biotinylated STIP1 mutant (S189A) was synthesized by the cell-free system and was used in the in vitro kinase assay.

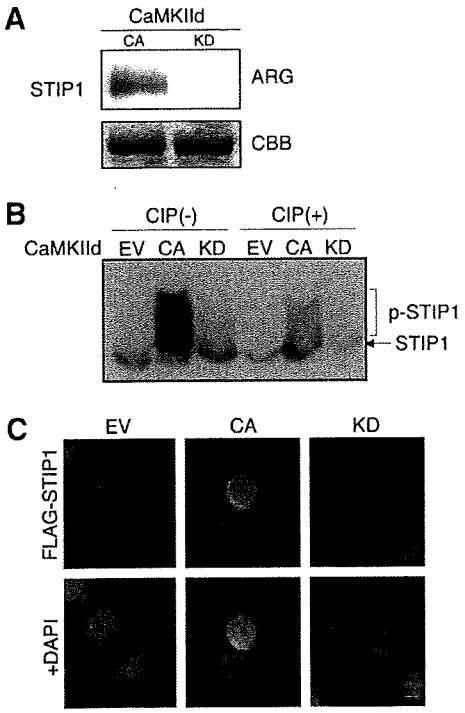

Fig. 4. In vivo phosphorylation of STIP1 and nuclear localization of STIP1 by expression of constitutively active CaMKIId. (A) Biotinylated STIP1 was purified using streptavidin-conjugated magnetic beads, then the beads were suspended in reaction mixture containing purified CA or KD CaMKIId mutants as described in Fig. 3. (B) HeLa cells were transfected with FLAG-STIP1 and co-transfected with empty vector (EV) or constitutive active (CA) or kinase dead (KD) CaMKII constructs. After 24 h, cell lysates were treated or untreated with calf intestine alkaline phosphatase (CIAP) and separated by phos-tag acrylamide gel, followed by immunoblotting with anti-FLAG antibody. (C) HeLa cells were transfected with FLAG-STIP1 and co-transfected with EV or CA or KD CaMKIId constructs. After 24 h, cells were fixed, permeabilized and immunostained with anti-FLAG (M2) antibody and subsequently stained with 4′,6-diamino-2-phenylindole (DAPI), and then subjected to fluorescent microscopy.

vector (EV) or CA or KD mutants of CaMKIId, After 24 h following transfection, cell lysates were subjected to phos-tag gel analysis. As indicated in Fig. 4B, significant band shift, indicative of phosphorylated STIP1, was observed in cells transfected with CA, but neither EV nor KD (left panel). This shift was significantly reduced when cell lysates were treated with calf intestine alkaline phosphatase (right panel), indicating that CaMKIId can phosphorylate STIP1 in vivo. We next address the biological effect of STIP1 phosphorylation by CaMKIId. Immunofluorescent analysis revealed that STIP1 is selectively localized at the nuclei in CA expressing cells, as detected by DAPI stain, while it was mainly localized in cytoplasm and cell periphery in EV or KD expressing cells (Fig. 4C). Cell viability and morphology were not significantly changed in transfected cells. The Ser189 in STIP1 was previously reported as a phosphorylation site of Casein kinase II (CKII). However, expression of EV and KD mutant showed cytoplasmic and cell-peripheral localization of STIP1 in the cell. Furthermore, treatment with specific CKII inhibitor (5,6-dichlorobenzimidazole 1-β-D-ribofuranoside) had no effect on the cytoplasmic distribution of mSTI1 [12]. Taken together, these data suggest that CKII in these cells may not be a crucial regulator of STIP1 localization to the nucleus. These results indicate that the phosphorylation of STIP1 by CaMKIId exerts the nuclear translocation of STIP1 for certain biological function.

4. Discussion

STIP1 interacts with Hsp70 and Hsp90 at its N and C termini in the cytoplasm as a co-chaperone, and can modulate the chaperone activities of these Hsps [18,19]. It is also known that STIP1 may be an important component in the oligomerization of heat-shock transcription factor (HSF1) complex in the nucleus [20]. STIP1 localizes predominantly cytoplasmic under normal growth conditions, and it might move between cytoplasm and nucleus under certain cell cycle conditions [12]. Phosphorylation of mSTI1, the mouse homologue of human STIP1, at Ser189 and Thr198 by cell cycle kinases (CKII and cdc2 in vitro, respectively) may modulate nuclear import and export in vivo [12]. In a recent report, STIP1 translocated to the nucleus in response to heat shock [21]. Interestingly, it has also been found that heat shock response was increased

concentration of the intercellular Ca^{2+} in a variety of cells [22]. These observations lead to speculation that CaMKIId might induce nuclear translocation of STIP1 in response to heat shock. In this study, we identified that the CaMKIId phosphorylated STIP1 at Ser189 in HeLa cells and also confirmed that co-transfection with CA-CaMKIId promotes STIP1 nuclear localization. The results suggest that calcium signals via CaMKIId may regulate subcellular localization of STIP1.

In the case of eIF4B, phosphorylation by S6KI, PKC, PKA, CKI, CKII and PAKI has been reported in vitro [13,14]. The known phosphorylation sites of human eIF4B are Ser93 [23], Ser422 [15], Ser425 [24], Ser498 [23] and Ser504 [23]. Ser597 phosphorylation is also known in the mouse homolog eIF4B [25]. The influence of phosphorylation on eIF4B is not well understood, but it is suggested that phosphorylation of Ser422 by S6KI interferes with translation initiation in vivo[15]. Although we confirmed that eIF4B was phosphorylated by CaMKIId in vitro, the phosphorylation site(s) and physiological role of CaMKIId phosphorylation remain to be elucidated.

In recent years, studies of phosphorylation signaling have evolved dramatically and various approaches have been tried to elucidate phosphorylation signaling pathways. However, identification of kinase substrates has been hampered by difficulties in synthesizing sufficient quantities of functionally active recombinant proteins for biochemical analysis. Although peptide screens allow rapid characterization of the preferred primary sequence for phosphorylation by a kinase, these assays are plagued by a potential lack of specificity. In this study, we attempted to screen CaMKIId substrates from HeLa cell extracts by using crude kinase expressed in the wheat germ cell-free system. Using this system, we have successfully identified STIP1 and eIF4B as new phosphorylation target proteins. This new strategy, which can use crude kinase for screening, provides a simple and easy way to facilitate analysis of substrates for protein kinases. Because of the utilization of natural substrates, substrate specificity is more similar to the physiological reaction than when using peptides and denatured proteins. In addition, the use of crude kinases in the screening not only facilitates preparation of the kinase of interest but also may decrease the risk of deactivation of kinases suffered by screens utilizing kinases with purification tags or which have gone through purification processes. In the method described here the number of candidate substrate spots could be increased by applying, for example, fluorescent staining or silver staining which are more sensitive than CBB staining. Overlap pH isoelectric point electrophoresis and use of phospho-protein enrichment columns may also be of use in increasing the number of candidates. Although our approach has proven effective, some issues still need to be addressed and these include: (i) ensuring that the protein kinase is in the active form. (ii) Phosphorylation cannot be detected when the protein has already been phosphorylated in the cell, even if it is a physiological substrate. (iii) Proteins that have a remarkably biased p*I* such as nuclear receptor are outside the range of isoelectric focusing. (iv) Low abundance proteins are very difficult to detect.

We have therefore confirmed that phosphorylation substrates of CaMKIId can be detected using cell-free synthesized crude kinase without any purification and that the wheat cell-free system could produce functionally active kinases. These experiments indicate that our simple approach based on a wheat cell-free system is a useful tool for easy screening for substrate proteins of protein kinases in cell extracts.

Acknowledgements: We thank Keizo Oka (Department of Bioscience, INCS, Ehime University) for culture of HeLa cell lines. This work was partially supported by the Special Coordination Funds for Promoting Science and Technology by the Ministry of Education, Culture, Sports, Science and Technology, Japan (Y.E. and T.S.).

References

[1] Clapham, D.E. (1995) Calcium signaling. Cell 80, 259–268.
[2] Hudmon, A. and Schulman, H. (2002) Structure-function of the multifunctional Ca^{2+}/calmodulin-dependent protein kinase II. Biochem. J. 364, 593–611.
[3] Singh, S., Powell, D.W., Rane, M.J., Millard, T.H., Trent, J.O., Pierce, W.M., Klein, J.B., Machesky, L.M. and McLeish, K.R. (2003) Identification of the p16-Arc subunit of the Arp 2/3 complex as a substrate of MAPK-activated protein kinase 2 by proteomic analysis. J. Biol. Chem. 278, 36410–36417.
[4] Ogasawara, T., Sawasaki, T., Morishita, R., Ozawa, A., Madin, K. and Endo, Y. (1999) A new class of enzyme acting on damaged ribosomes: ribosomal RNA apurinic site specific lyase found in wheat germ. EMBO J. 18, 6522–6531.
[5] Madin, K., Sawasaki, T., Ogasawara, T. and Endo, Y. (2000) A highly efficient and robust cell-free protein synthesis system prepared from wheat embryos: plants apparently contain a suicide system directed at ribosomes. Proc. Natl. Acad. Sci. USA 97, 559–564.
[6] Sawasaki, T., Hasegawa, Y., Tsuchimochi, M., Kamura, N., Ogasawara, T., Kuroita, T. and Endo, Y. (2002) A bilayer cell-free protein synthesis system for high-throughput screening of gene products. FEBS Lett. 514, 102–105.
[7] Sawasaki, T., Ogasawara, T., Morishita, R. and Endo, Y. (2002) A cell-free protein synthesis system for high-throughput proteomics. Proc. Natl. Acad. Sci. USA 99, 14652–14657.
[8] Sawasaki, T., Hasegawa, Y., Morishita, R., Seki, M., Shinozaki, K. and Endo, Y. (2004) Genome-scale, biochemical annotation method based on the wheat germ cell-free protein synthesis system. Phytochemistry 65, 1549–1555.
[9] Endo, Y. and Sawasaki, T. (2006) Cell-free expression systems for eukaryotic protein production. Curr. Opin. Biotechnol. 17, 373–380.
[10] Sawasaki, T., Kamura, N., Matsunaga, S., Saeki, M., Tsuchimochi, M., Morishita, R. and Endo, Y. (2008) Arabidopsis HY5 protein functions as a DNA-binding tag for purification and functional immobilization of proteins on agarose/DNA microplate. FEBS Lett. 582, 221–228.
[11] Ryo, A., Togo, T., Nakai, T., Yamaguchi, A., Suzuki, K., Perrem, K., Hirayasu, Y., Liou, Y.C. and Aoki, I. (2006) The prolyl-isomerase Pin1 accumulates in the Lewy bodies of Parkinson's disease and facilitates the formation of α-synuclein inclusions. J. Biol. Chem. 281, 4117–4125.
[12] Longshaw, V.M., Chapple, J.P., Balda, M.S., Cheetham, M.E. and Blatch, G.L. (2004) Nuclear translocation of the Hsp70/Hsp90 organizing protein mSTI1 is regulated by cell cycle kinases. J. Cell. Sci. 117, 701–710.
[13] Morley, S.J. and Traugh, J.A. (1989) Phorbol esters stimulate phosphorylation of eukaryotic initiation factors 3, 4B, and 4F. J. Biol. Chem. 264, 2401–2404.
[14] Morley, S.J. and Traugh, J.A. (1990) Differential stimulation of phosphorylation of initiation factors eIF-4F, eIF-4B, eIF-3, and ribosomal protein S6 by insulin and phorbol esters. J. Biol. Chem. 265, 10611–10616.
[15] Raught, B., Peiretti, F., Gingras, A.C., Livingstone, M., Shahbazian, D., Mayeur, G.L., Polakiewicz, R.D., Sonenberg, N. and Hershey, J.W.B. (2004) Phosphorylation of eucaryotic translation initiation factor 4B Ser422 is modulated by S6 kinases. EMBO J. 23, 1761–1769.
[16] Rush, J., Moritz, A., Lee, K.A., Guo, A., Goss, V.L., Spek, E.J., Zhang, H., Zha, X.M., Polakiewicz, R.D. and Comb, M.J. (2004) Immunoaffinity profiling of tyrosine phosphorylation in cancer cells. Nat. Biotechnol. 23, 94–101.

[17] Kinoshita, E., Kinoshita-Kikuta, E., Takiyama, K. and Koike, T. (2006) Phosphate-binding tag, a new tool to visualize phosphorylated proteins. Mol. Cell. Proteomics 5, 749–757.
[18] Chen, S. and Smith, D.F. (1998) Hop as an adaptor in the heat shock protein 70 (Hsp70) and Hsp90 chaperone machinery. J. Biol. Chem. 273, 35194–35200.
[19] Odunuga, O.O., Longshaw, V.M. and Blatch, G.L. (2004) Hop: more than an Hsp70/Hsp90 adaptor protein. Bioessays 26, 1058–1068.
[20] Bharadwaj, S., Ali, A. and Ovsenek, N. (1999) Multiple components of the HSP90 chaperone complex function in regulation of heat shock factor 1 *in vivo*. Mol. Cell. Biol. 19, 8033–8041.
[21] Daniel, S., Bradley, G., Longshaw, V.M., Söti, C., Csermely, P. and Blatch, G.L. (2008) Nuclear translocation of the phosphoprotein Hop (Hsp70/Hsp90 organizing protein) occurs under heat shock, and its proposed nuclear localization signal is involved in Hsp90 binding. Biochim. Biophys. Acta 1783, 1003–1014.
[22] Gong, K.J. and Tsokos, G.C. (1996) Cell signaling and heat shock protein expression. J. Biomed. Sci. 3, 379–388.
[23] Beausoleil, S.A., Jedrychowski, M., Schwartz, D., Elias, J.E., Villen, J., Li, J., Cohn, M.A., Cantley, L.C. and Gygi, S.P. (2004) Large-scale characterization of HeLa cell nuclear phosphoproteins. Proc. Natl. Acad. Sci. USA 101, 12130–12135.
[24] Kim, J.E., Tannenbaum, S.R. and White, F.M. (2005) Global phosphoproteome of HT-29 human colon adenocarcinoma cells. J. Proteome. Res. 4, 1339–1346.
[25] Ballif, B.A., Villén, J., Beausoleil, S.A., Schwartz, D. and Gygi, S.P. (2004) Phosphoproteomic analysis of the developing mouse brain. Mol. Cell. Proteomics 3, 1093–1101.

FEBS Letters 582 (2008) 2737–2744

DNA-binding profiling of human hormone nuclear receptors via fluorescence correlation spectroscopy in a cell-free system

Tamiyo Kobayashi[a,b], Yoshiko Kodani[a], Akira Nozawa[a,c], Yaeta Endo[a,c,*], Tatsuya Sawasaki[a,c,*]

[a] *Cell-Free Science and Technology Research Center, and The Venture Business Laboratory, Ehime University, 3 Bunkyo-cho, Matsuyama, Ehime 790-8577, Japan*
[b] *Life Science Group, Olympus Corp., 2-3 Kuboyama-cho, Hachioji, Tokyo 192-8512, Japan*
[c] *RIKEN Genomic Sciences Center, 1-7-22 Suehiro-cho, Tsurumi, Yokohama 230-0045, Japan*

Received 11 April 2008; revised 1 July 2008; accepted 1 July 2008

Available online 11 July 2008

Edited by Paul Bertone

Abstract The nuclear hormone receptors (NHRs), a family of transcription factors, bind directly to the hormone response elements (HREs) to regulate gene expression. In this study, we describe a comprehensive NHR–HRE profiling analysis with a new high-throughput DNA binding assay system utilizing wheat germ cell-free protein production and fluorescence correlation spectroscopy (FCS). This approach revealed NHR binding to natural response elements and new heterodimeric NHR–HRE bindings. We analyzed 408 possible binding combinations between 34 human NHRs and 12 different HREs, and identified 205 NHR–HRE binding combinations, 124 of which have not been previously reported. Thus, this study provides a novel biochemical classification of the human NHRs, as well as describing a novel approach to the large-scale analysis of DNA–protein interactions.

Keywords: Cell-free protein production; DNA-binding profiling; Fluorescence correlation spectroscopy; Nuclear hormone receptor; Hormone response elements; Biochemical annotation

1. Introduction

One-third of the 48 nuclear hormone receptors (NHRs) found on the human genome are orphan receptors as their ligands are not known [1]. The NHR superfamily of transcription factors directly activates or represses target genes by binding to the hormone response elements (HREs). Thus, these proteins play a central role in many biological processes such as cell growth and differentiation, embryonic development, and metabolic homeostasis in metazoan organisms. The HREs, in which a 6-bp long sequence constitutes the core recognition motif, are located in the regulatory region of the gene. Although some monomeric receptors can bind to a single hexameric recognition motif, most receptors bind as homodimers or heterodimers to the HREs composed typically of two core hexameric motifs. For dimeric HREs, the half-sites can be configured as direct repeats (DR) or as palindromes (Pal). The binding specificity of the NHR varies depending on the length of the spacer region between the two HRE half-sites [2].

Fluorescence correlation spectroscopy (FCS) is an advanced technology that is used for measuring the translational diffusion coefficients of molecules in solutions [3,4]. FCS technology is ideal for measuring the molecular interactions because the translational diffusion coefficient of a molecule depends on its molecular weight, structure and number. We recently developed an automated FCS system suitable for applications ranging from the high-throughput analyses to complex studies of molecular interactions, and using this system we have previously described a binding assay for the DNA-transcriptional factors such as NF-κB in crude cellular extracts [5]. In contrast to the electrophoretic mobility shift assay (EMSA), the binding assay using the FCS technique contained steps that are less time consuming, and consequently, the measurements can be carried out within a very short period of time (10–20 s per sample). Thus, an assay based on FCS could facilitate the analysis of DNA–protein interactions tens of times faster than EMSA.

Wheat germ extract cell-free protein synthesis technology has made it possible to produce a wide range of difficult-to-express proteins, which includes prokaryotic, eukaryotic and artificial proteins, in naturally folded states [6]. We developed a high-throughput, genome-scale protein synthesis method based on the wheat germ extract cell-free expression system, and using this system we have successfully synthesized 34 different types of human NHRs. We report here a comprehensive method for the biochemical analysis of binding between 34 different human NHRs and 12 different DNA response elements. In addition, this analysis reveals instances of new heterodimeric bindings of the NHRs.

2. Materials and methods

2.1. General

Details of the following procedures have been either described or cited previously [6,7]: generation of DNA template by PCR using split-primers, synthesis of mRNA, protein synthesis in parallel, estimation of amount of protein synthesized by means of densitometric scanning of the Coomassie brilliant blue® (CBB)-stained band and autoradiography. The wheat germ extract was purchased from Cell-Free Sciences, Co. (Yokohama, Japan). Autoradiography was analyzed by BAS-2500 (Fuji film, Tokyo, Japan). Reagents used in this study were described previously [6].

*Corresponding authors. Address: Cell-Free Science and Technology Research Center, Venture Business Laboratory, Ehime University, 3 Bunkyo-cho, Matsuyama, Ehime 790-8577, Japan. Fax: +81 89 927 9941 (T. Sawasaki).
E-mail addresses: yendo@eng.ehime-u.ac.jp (Y. Endo), sawasaki@eng.ehime-u.ac.jp (T. Sawasaki).

0014-5793/$34.00
doi:10.1016/j.febslet.2008.07.003

2.2. DNA-template construction for transcription

The DNA templates for transcription were obtained by using the split primer PCR technique using gene specific primers (S1-sense primer shown in Supplementary Table S1). PCR conditions and transcription were described previously [6].

2.3. Cell-free translation

Cell-free translation is based on a bilayer diffusion system that consists of a translation mixture and substrate mixture [7] including 10 μM zinc acetate. The translation reaction was carried out in 96-well titer plates. Each well containing 25 μl of the translation mixture was then carefully overlaid with 125 μl of the substrate mixture. The plate was incubated at 26 °C for 18 h.

2.4. Preparation of the double-stranded DNA

Sequences of the single-stranded DNAs used in this study are listed in Supplementary Table S2. Each DNA fragment was amplified with the common primer labeled with TAMRA and one of the non-labeled primers using the Ampli-Taq Gold kit. The PCR products were electrophoresed in 15% polyacrylamide, and the target TAMRA-labeled double-stranded DNA was excised from the gel and purified with QIAquick extraction kit (Qiagen, Düsseldorf, Germany). For natural response elements, the double-stranded DNA was prepared by annealing both oligonucleotides in 10 mM TE buffer (pH 8.0) containing 0.1 M sodium chloride. The reaction mixture was hydrolyzed stepwise in the $3' \rightarrow 5'$ direction by exonuclease I to remove the single-strand DNA and then the hydrolyzed nucleotides, free dyes, and salts were removed by using MERmaid SPIN (Qbiogen, Carlsbad, CA).

2.5. DNA-binding assay using the fluorescence correlation spectroscopy (FCS)

For detecting NHR–HRE binding, 5 μl of the translational mixture, including the synthesized protein product, was incubated at 30 °C for 30 min in the presence of 1 nM of TAMRA-labeled DNA. The reaction was carried out in a total volume of 24 μl reaction mixture containing 50 mM KCl, 2 mM $MgCl_2$, 20 mM Hepes-KOH (pH 7.8), 1 mM DTT, 0.1 mM EDTA, 100 μg/ml BSA, 5% glycerol and 0.2 mg/ml poly(dI–dC). The samples were sequentially and automatically loaded onto a 384-well glass-bottomed microplate, and FCS measurements were performed using the single-molecule fluorescence detection system, MF20 (Olympus, Tokyo, Japan). For hormone-dependent glucocorticoid receptor (GR) binding, synthesized GR (15 μl) was incubated with or without 5 nM cortisol at 30 °C for 30 min. For heterodimerization, 2.5 μl of retinoid X receptor (RXR) γ was mixed with 2.5 μl of vitamin D receptor (VDR), peroxisome proliferator-activated receptor (PPAR) α, PPARβ, or PPARγ. Fluorescence was measured using a He–Ne laser (excitation wavelength 543 nm) and a 580DF30 filter. The optical system of the device was automatically adjusted for each measurement. All experiments were performed under identical conditions with a data acquisition time of 15 s per measurement, and were repeated five times per sample.

2.6. Definition of positive DNA-binding ability for NHR

In the FCS assay, the diffusion time of a labeled molecule in a laser-illuminated region is measured. The diffusion time of a molecule can be theoretically calculated from its molecular weight. Here, DNA is assumed to conform to a spherical shape and its molecular weight is calculated according to 662 Da per base-pair; moreover, under saturated conditions, all the TAMRA-labeled DNA in the reaction solution is assumed to form a monomer or dimer. The diffusion time correlates with the molecular weight of the labeled molecule. When NHR binds to labeled DNA, the molecular weight of the NHR–DNA complex becomes higher than the DNA alone. In general, because the mobility of a molecule in solution dependents on its molecular weight, the mobility of the NHR–DNA complex becomes slower than DNA alone. Consequently, the slower protein–DNA complex exhibits longer diffusion time [5].

In the FCS system, therefore, NHR binding to DNA can be detected by prolonged diffusion times. This time difference is also calculated from the molecular weights of DNA and NHR complexes, assuming that each NHR forms a monomer on the core motif and forms a homodimer on DR or Pal. By comparing the results of the FCS analysis with those derived from EMSA measurements carried out in parallel, we observed that the DNA–NHR complexes were actually detected in EMSA when the prolongation of diffusion time is 30% or higher than the theoretical values. Consequently, we selected a threshold value for the binding degree, and defined the DNA-binding ability of an NHR as positive when the binding degree for the pair was 30% or higher. From a total of 408 possible binding combinations, 145 demonstrated positive binding by EMSA, whereas 140 were positive (i.e., exhibiting a binding degree 30% or higher than the threshold) by FCS.

Other materials and methods used are described in the supplementary data.

3. Results and discussion

3.1. Binding of NHRs produced by the wheat cell-free system to human natural response elements using FCS

To investigate whether NHRs synthesized by the wheat cell-free system can bind human natural response elements, we prepared the human natural response elements of apolipoprotein A-I (ApoA-I) [8] and medium-chain acyl coenzyme A dehydrogenase (MCAD) genes [9] by annealing the respective synthetic oligonucleotides (DNA sequences listed in Supplementary Table S3). ApoA-I is a major protein component of high-density lipoprotein (HDL), and plays an important role in the reverse cholesterol transport pathway. The regulatory element (−220/−190) on the ApoA-I gene contains DR of the PuGTTCA motif separated by 2 bp, and is recognized by the RXRα homodimer and RXRα/retinoic acid receptor (RAR) α heterodimer [8].

Using the FCS assay system we confirmed the binding of RXRα to the ApoA-I regulatory element, but not to the thyroid hormone receptor (TR) α regulatory element (a negative control) (Fig. 1A). Nuclear receptor response element (NRRE)-1 (−341/−307), a pleiotropic element present in the MCAD gene promoter [9], is known to interact with a number of NHRs including the RXR and estrogen related receptor (ERR). Maehara et al. previously reported that the ERR, but not the PPAR, bound to the NRRE-1 as a homodimer or as two independent monomers [10]. Consistent with this report, we also found that the ERRγ bound to the NRRE-1, whereas the PPARα (a negative control) did not (Fig. 1B).

To elucidate the hormone-mediated transcriptional network, it is important to investigate the ligand-binding as well as the DNA-binding specificities of the NHRs. We therefore examined the effects of the ligand on DNA–GR binding, finding that binding of GR to the cytochrome P450 2C9 (CYP2C9) gene promoter element was enhanced by cortisol as one of the glucocorticoids (Fig. 1C). In this way, FCS is able to contribute to the analysis of not only the NHR–HRE molecular interactions but also the ligand-NHR or DNA–NHR-ligand molecular interactions. These results suggest that the high-throughput method described here could be used to identify the natural response elements found in the promoters and enhancers, and to screen the hormone ligand to further investigate the effects on the DNA binding. Moreover, FCS represents a potentially general technique for drug selection, to identify candidates that interfere with or modify particular binding interactions.

3.2. Production of 34 human NHR proteins by the wheat germ extract cell-free system

Thirty-four NHR proteins were synthesized using the wheat germ extract cell-free system supplement with zinc ion. The

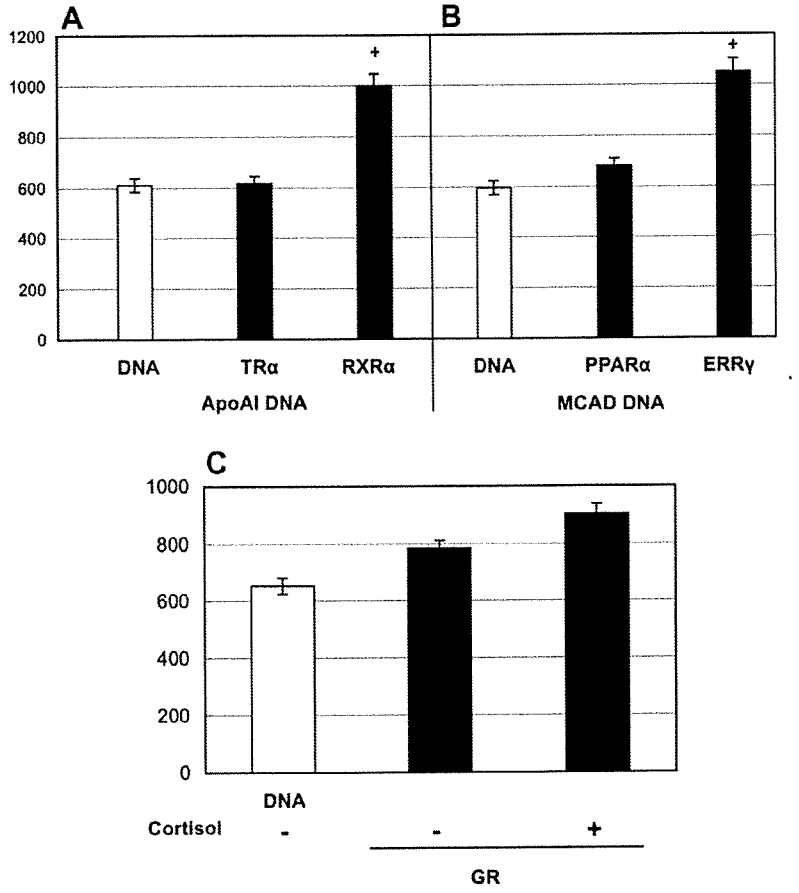

Fig. 1. FCS detection of DNA-binding specificities of RXRα and ERRγ, and hormone response of GR to the natural human DNA response elements. Binding of (A) TRα (negative control) or RXRα to the binding element on the ApoA-I gene, and (B) PPARα (negative control) or ERRγ to the binding element on the MCAD gene were examined by FCS. Binding experiments were performed using either of the synthesized protein products. The symbol "+" represents a diffusion time ratio of 30% and higher. (C) Binding of GR to the CYP2C9 gene promoter element was enhanced by cortisol as one of the glucocorticoids. The vertical axis shows the diffusion time (μs) of TAMRA-labeled DNA (1 nM) or NHR–HRE complexes in the reaction solution. Error bars represent the S.D. of five measurements.

NHR products, synthesized in the presence of radioisotope-labeled amino acid (^{14}C-Leu), were confirmed by analyzing autoradiographs of the respective SDS–polyacrylamide gels following electrophoresis. Each protein appeared as a single band on the autoradiogram (data not shown). Proteins were quantified by incorporation of ^{14}C-Leu, and the average yield was found to be approximately 3.5 ± 1.4 μg of protein per 100 μl of reaction mixture. We also checked the solubility of the each product as previously reported [7], and found that 65 ± 25% each product was soluble. The yields and solubilities of each synthesized protein are shown in Supplementary Table S4.

3.3. Binding analysis of 34 human NHRs to core, DR and Pal motifs using FCS

We used the automated FCS technique to systematically study the DNA-binding properties of 34 NHRs. In this binding assay, a given NHR protein product was mixed with a fluorescence-labeled DNA probe. Diffusion time of the labeled DNA in the reaction mixture was measured using FCS. Prolongation of diffusion time in reaction solution, compared with the control value, indicates NHR–HRE complex formation. Each diffusion time was categorized into 10 different levels (from 1 to 10) according to its binding degree, i.e. the ratio of the actual measurement value to the theoretically expected value (see Section 2.6). The double-stranded DNAs used as probes are listed in Supplementary Table S2.

In addition, we analyzed the interactions between the 34 NHRs and 12 NHEs by EMSA to confirm their DNA-binding abilities. Fig. 2 includes typical EMSA results. Comparisons of the results obtained from the FCS and EMSA analyses suggested that the NHR–HRE pairs whose diffusion times belonged to the scored categories 4 through 10, as determined from the FCS analysis, formed NHR–HRE complexes on EMSA. In contrast, the NHR–HRE pairs whose diffusion times belonged to the categories 1 through 3 as determined from FCS failed to form NHR–HRE complexes on EMSA. Thus, we determined that a diffusion time ratio of 30% and higher by FCS analysis indicates positive NHR–HRE binding.

3.4. Evaluation of NHR–HRE binding data

Table 1 summarizes the binding results of the 34 NHRs as shown in Fig. 2. Twenty-four out of thirty-four different NHRs bound to a DNA element in a ligand-independent manner. Several NHRs, such as Rev-erbAβ and tailless nuclear hormone receptor (TLX), bound to DNA only when higher amounts (15 μl) of the synthesized protein was used in the as-

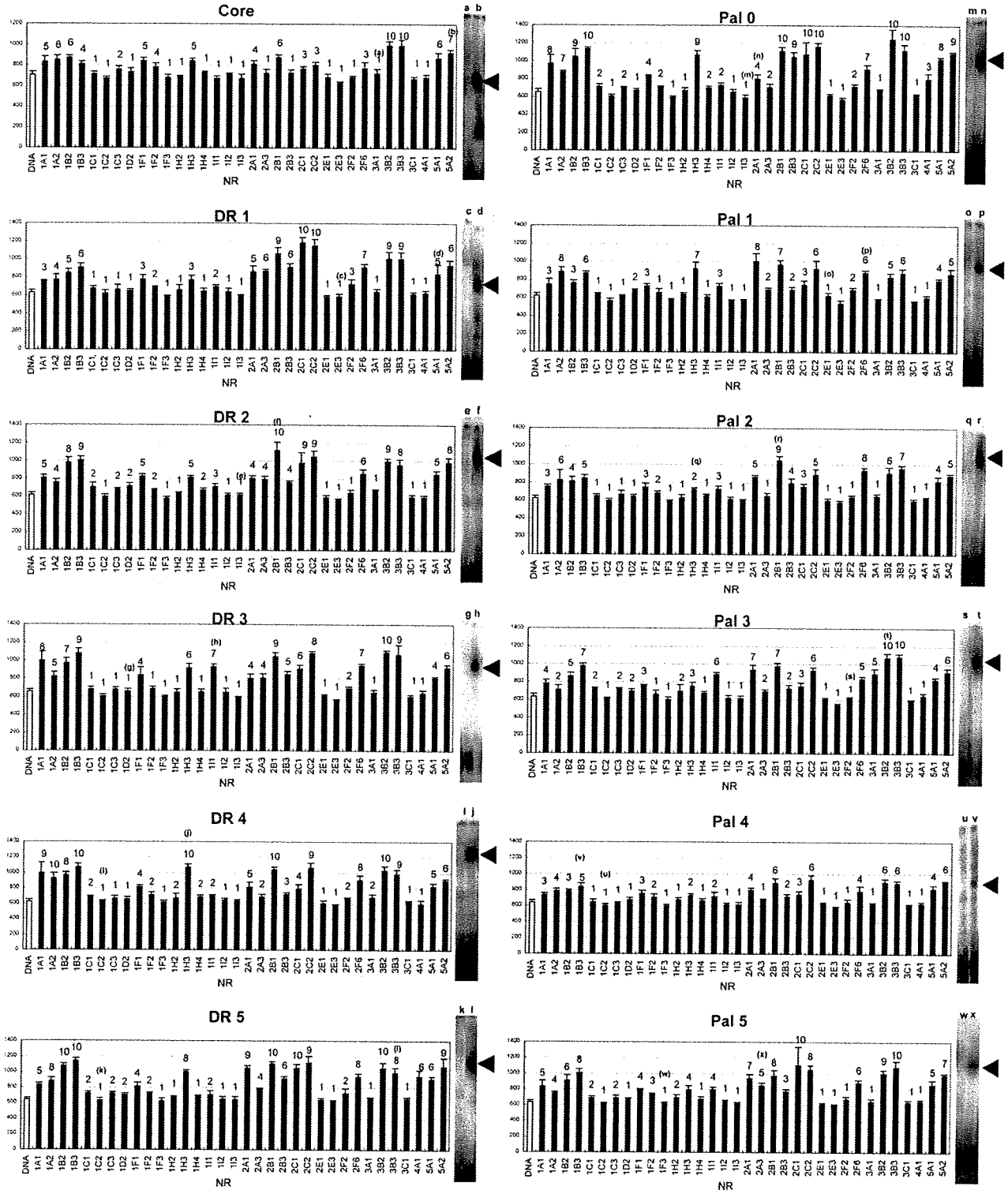

Fig. 2. Detection of NHR–HRE interactions with FCS. The vertical axis shows diffusion time (μs) of the TAMRA-labeled DNA or NHR–HRE complex in the reaction solution. Results from the representative EMSA experiments were also shown (autoradiograms). Numbers in the parentheses correspond to the representative EMSAs. Arrowheads indicate specific NHR–HRE complexes. Open bar indicates a negative control where the synthesized protein product was prepared from the plasmid lacking the DNA-binding domain. Error bars represent the S.D. over five measurements. Labels 1 through 10 indicate the diffusion time ratios of the actual measurement values to the theoretically expected values: 1 indicates less than 10%, and 2, >10–20%; 3, >20–30%; 4, >30–40%; 5, >40–50%; 6, >50–60%; 7, >60–70%; 8, >70–80%; 9, >80–90%; and 10, >90%. Core, DR and Pal indicate the DNA probes used in this experiment.

Table 1
NHR–HRE binding profiling by wheat cell-free based FCS

Genes	Names	Core	DR 1	DR 2	DR 3	DR 4	DR 5	Pal 0	Pal 1	Pal 2	Pal 3	Pal 4	Pal 5
NR1A1	TRα	+* 16	-	+* 16	+* 17	+* 16,17	+* 17	+* 16,17	-	-	+* 16,18	-* 17	+* 16
NR1A2	TRβ	+* 2,18	+	+* 2	+* 19	+* 19	+* 2,19	+* 2,19,20	+	+	+* 2,18	+	+
NR1B2	RARβ	+* 2,18	+	+* 2	+	+	+* 2	+* 2	-	+	+* 2,18	-	+
NR1B3	RARγ	+* 18	+	+	+	+	+	+	+	+	+* 18	+	+
NR1C1	PPARα	-	-* 11	-	-	-	-	-	-	-	-	-	-
NR1C2	PPARβ	-	-	-	-	-	-	-	-	-	-	-	-
NR1C3	PPARγ	-	-	-	-	-	-	-	-	-	-* 12	-	-
NR1D2	Rev-erbAβ	-* 3	-	+* 3	-	-	-	(+)	(+)	-	(+)	(+)	-
NR1F1	RORα	+* 21,22	(+)* 21	+* 21	+	+	+	+* 22	(+)	(+)	(+)	(+)	+
NR1F2	RORβ	+	-	-	-	-	-	-	-	-	-	-	-
NR1F3	RORγ	-	-	-	-	-	-	-	-	-	-	-	-
NR1H2	LXRβ	-	-	-	-	-	-	-	-	-	-	-	-
NR1H3	LXRα	+	-	+	+	+* 23	+	+	+	-	-	-	+
NR1H4	FXR	-	-	-	-	-	-	-	-	-	-	-	-
NR1I1	VDR	-	-	-	+* 15,19	-* 19	(+)* 19	(+)	-	(+)	+	-	+
NR1I2	PXR	-	-	-	-	-	-	-	-	-	-	-	-
NR1I3	CAR	-	-	-	-	-	-	-	-	-	-	-	-
NR2A1	HNF4α	+* 24	+* 24	+* 24	+	+	+	+	+	+	+	+	+
NR2A3	HNF4γ	-	+	+	+	(+)	+	-	(+)	-	-	-	+
NR2B1	RXRα	+	+* 11,17	+* 17	+* 17	+* 17,25	+* 17	+* 26	+* 17	+* 17	+* 17	+* 17	+* 17
NR2B3	RXRγ	-	+	+	+	-* 25	+	+	-	(+)	-	-	(+)
NR2C1	TR2	(+)	+* 7	+* 7	+* 7	+* 7	+* 7	+	(+)	-	(+)	-	+
NR2C2	TR4	(+)	+* 6	+* 6	+* 6	+* 6	+* 6	+	+	+	+* 6	+	+
NR2E1	TLX	-	-	-	-	-	-	-	(+)	-	-	-	(+)
NR2E3	PNR	-	-	-	-	-	-	-	-	-	-	-	-
NR2F2	COUP-TFII	-	(+)* 8	(+)* 27	(+)* 27	(+)* 8,27	(+)* 27	(+)* 8	(+)* 28	-	-	-	-
NR2F6	EAR2	-	+* 27	+	+	+* 20	+	+* 20	+	+	+	-	+
NR3A1	ERα	-	-	-	-	-	-	-* 6	-	-	+* 6,18	-	-
NR3B2	ERRβ	+* 29	+	+	+	+	+	+	+	+	+	+	+
NR3B3	ERRγ	+* 5,19	+* 5	+* 5	+* 5	+* 5	+* 5	+* 5	+* 5	+* 5	+* 5	+* 5	+* 5
NR3C1	GR	-	-	-	-	-	-	-	-	-	-	-	-
NR4A1	NGFI-Bα	-* 30	-	-	-	-	+	(+)	-	-	-	-	-
NR5A1	SF-1	+* 1	+	+	+	+	+	+	+	+	+	+	+
NR5A2	LRH-1	+* 1	+	+	+	+	+	+	+	+	+	+	+

Five μl of synthesized protein was used in this binding assay. The symbols "+" and "−" over the theoretically expected value calculated from the estimated molecular mass of the DNA–NHR complex under saturated condition where all TAMRA-labeled oligonucleotides were bound to the NHR of 30% and higher, and less than 30%, respectively. (+) Symbol in the parentheses indicates that while there was no measurable DNA–NHR interaction using 5 μl of the synthesized protein, a DNA–NHR interaction was observed when 15 μl of the synthesized protein was used in the reaction mixture. Asterisks (*) represent DNA–NHR interactions which were previously reported and the numbers refer to the respective references in the Supplementary data.

say, suggesting they have low DNA binding affinities. We examined 408 different NHR–HRE combinations (monomers and/or homodimers) for binding using the FCS-based assay, and consequently identified 205 different NHR–HRE interactions, 124 of which were novel and 81 that were previously reported (Table 1). However, eight previously reported NHR–HRE interactions (TRα-Pal4, PPARα-DR1, PPARγ-Pal3, Rev-erbAβ-core, VDR-DR4, RXRγ-DR4, ERα-Pal0, and NGFI-Bα-core) were not among the 205 NHR–HRE interactions reported in this study. One possible explanation for this discrepancy is that these eight interactions have used slightly different DNA fragments in the flanking and spacer sequences although the core sequence is the same. Because the significance of sequences around the core region is known [11,12], the interactions may also recognize flanking and/or spacer sequences in DNA fragment used.

The second explanation for the observed difference might lie in the requirement of a co-factor or ligand dependency. Almost all the previously reported NHR–HRE binding assays were performed using animal-derived protein expression systems such as rabbit reticulocyte lysate (PPARα), baculovirus-infected insect cell lysate (PPARγ and RXRγ) or cultured mammalian cell lysates (Rev-erbAβ, VDR, ERα, and NGFI-Bα). Although orphan receptors such as Rev-erbAβ and NGFI-Bα also exist among these eight combinations, these cell lysates might contain ligands and/or other essential factors for their DNA binding. This possibility is least likely in our assay system however, because the wheat germ extract is obviously of plant origin.

A third reason might be due to the nature of the protein (e.g., partial DNA-binding domain, full-length, and glutathione *S*-transferase- or FLAG-tagged proteins) used in the binding assay. Mader et al. reported that the DNA-binding domain of TR bound to the DR2 and Pal4 although the full-length TR did not bind to either DNA element [13]. We have also found that the full-length TRα did not bind to the Pal4 in our assay (Fig. 2), an observation that is consistent with that of Mader et al. In previous reports, FLAG- and HA-tagged proteins were used in the binding assay of PPARγ [11] and ERα [5], respectively. Because a full-length and non-tagged NHR protein is the original form in the cell, we believe that our assay (using a library of full-length NHRs) will provide more useful information than currently available assay systems for studying the NHR–HRE interaction.

3.5. Screening of binding partner forming heterodimers with RXRγ

RXRs are known to be promiscuous dimerization partners for a large number of NHRs, and their dimerization partners include themselves, RAR, VDR, TR, PPAR and other orphan receptors [1]. We next screened for binding of RXRγ heterodimers to DR4 and Pal3. To examine whether RXRγ heterodimerizes with VDR, PPARα, PPARβ and PPARγ, equal amounts of synthesized RXRγ and one of the four NHRs (VDR, PPARα, PPARβ or PPARγ) were mixed with each test DNA element and analyzed by FCS. We found that RXRγ heterodimerized with VDR on both DR4 and Pal3 (Fig. 3A and B). Yen et al. previously demonstrated RXR/VDR heterodimerization on DR4 [14], but RXR/VDR heterodimerization on Pal3 is a new finding. Our study also showed that the VDR bound to Pal3 as a homodimer (Fig. 3B, see also Fig. 2 and Table 1). Therefore, it is possible that the mixture of RXRγ and

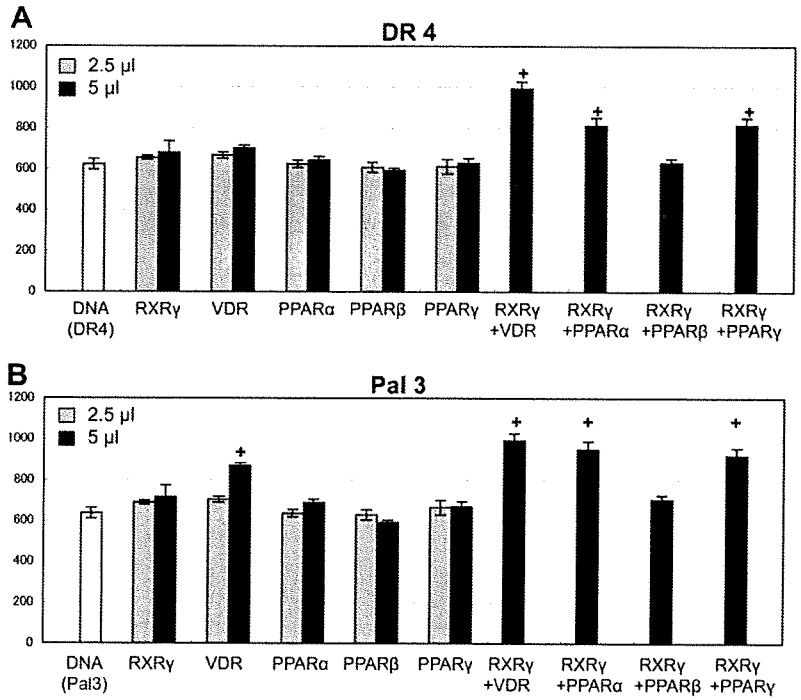

Fig. 3. DNA-binding abilities of the RXRγ/VDR, RXRγ/PPARα, RXRγ/PPARβ and RXRγ/PPARγ heterodimers. Binding of the RXRγ/VDR, RXRγ/PPARβ and RXRγ/PPARγ heterodimers with (A) DR4 and (B) Pal3 were examined by FCS. The vertical axis shows the diffusion time (μs) of the TAMRA-labeled HRE or NHR–HRE complex in the reaction solution. The symbol "+" represents a diffusion time ratio of 30% and higher. Error bars represent the S.D. of four measurements.

VDR might be forming both RXRγ/VDR heterodimers and VDR homodimers on Pal3.

In a systematic binding study using the DR elements with various spacers (DR0–DR5), it was previously shown that the RXR/PPAR heterodimer bound with the highest affinity to DR1 and with lesser affinities to DR0 and DR2 [15]. In addition, Okuno et al. reported that the RXR/PPARγ heterodimer bound to Pal3 [11]. In the present study, we found that RXRγ formed heterodimers with PPARα and PPARγ not only on Pal3 but also on DR4. However, our results showed that the RXRγ did not form a heterodimer with PPARβ on either DR4 or Pal3. Although PPARα and PPARγ did not bind to any DNA element as a homodimer (Fig. 2 and Table 1), they were able to recognize DNA sequences by forming heterodimers with RXRγ. Like PPARα and PPARγ, VDR was able to bind to DR4 as a VDR/RXR heterodimer, but not as a VDR homodimer.

3.6. Biochemical classification of human NHRs by DNA-binding profiling

We examined 408 different combinations for binding between DNA and NHRs (monomers and/or homodimers), and consequently detected 205 binding combinations of which 124 are new and 81 reported previously (Table 1). Based on the results of our binding assay, we classified all 34 NHRs into four groups (Fig. 4): (A) NHRs bound to all of the tested DNA elements with AGGTCA sequence (group A), (B) NHRs bound to two or more DR and/or Pal DNA elements (group B), (C) NHRs bound to only one type of DNA element (group C), and (D) NHRs not bound to any one of the DNA elements tested (group D). The NHRs belonging to group B were further classified into sub-groups based on their binding specificities to Core, DR and Pal (Fig. 4B-1, -2 and -3, respectively). Even though the NHRs in group D did not bind any of the tested DNA elements, several were able to form heterodimers with RXR or other receptors as described above. Although GR did not bind to any of the 12 DNA elements used in this study, it did bind to its response region in the human natural element (Fig. 1C) in our assay. Thus, we believe that some of the group D NHRs may recognize other HREs.

We compared these DNA-binding specificity-based clusters with the conventional sequence/domain conservation-based clusters. We found that the DNA sequences and the binding specificities of the group A members ERRβ and steroidogenic factor-1 (SF-1) were similar to the ERRγ and liver receptor homolog-1 (LRH-1), respectively. But, the DNA sequences of ERRβ (or ERRγ) are quite different from that of the SF-1 (or LRH-1) regardless of their similar binding specificities. Thus, our biochemical classification showed that similarity in the DNA sequence does not necessarily mean similarity in DNA-binding specificity. This approach, which categorizes NHRs in different clusters (clusters are separated by bold lines in Fig. 4), could bring new perspectives to NHRs, as the classification of the NHRs based on their DNA-binding specificities and not on their conserved sequences and/or domains. For example, our results suggest that the group A NHRs may be involved in regulating the same gene even though they bind to different hormones.

In conclusion, we propose that the combination of the high-throughput, genome-scale protein production method based

A Group A Binding to all the DNA elements with AGGTCA

Nuclear receptor	Core	DR1	DR2	DR3	DR4	DR5	Pal0	Pal1	Pal2	Pal3	Pal4	Pal5
1A2 TRβ	○	○	○	○	○	○	○	○	○	○	○	○
1B3 RARγ	○	○	○	○	○	○	○	○	○	○	○	○
1F1 RORα	◉	◉	◉	◉	◉	◉	◉	◉	◉	◉	◉	◉
2A1 HNF4α	○	○	○	○	○	○	○	○	○	○	○	○
2B1 RXRα	○	○	○	○	○	○	○	○	○	○	○	○
2C2 TR4	○	○	○	○	○	○	○	○	○	○	○	○
3B2 ERRβ	◉	◉	◉	◉	◉	◉	◉	◉	◉	◉	◉	◉
3B3 ERRγ	◉	◉	◉	◉	◉	◉	◉	◉	◉	◉	◉	◉
5A1 SF-1	○	○	○	○	○	○	○	○	○	○	○	○
5A2 LRH-1	○	○	○	○	○	○	○	○	○	○	○	○

C Group C Binding to the only one element

Nuclear receptor	Core	DR1	DR2	DR3	DR4	DR5	Pal0	Pal1	Pal2	Pal3	Pal4	Pal5
1F2 RORβ	◉											
3A1 ERα										○		

D Group D Not binding to any DNA elements

Nuclear receptor	Core	DR1	DR2	DR3	DR4	DR5	Pal0	Pal1	Pal2	Pal3	Pal4	Pal5
1C1 PPARα												
1C2 PPARβ												
1C3 PPARγ												
1F3 RORγ												
1H2 LXRβ												
1H4 FXR												
1I2 PXR												
1I3 CAR												
2E3 PNR												
3C1 GR												

B Group B Binding to two and more core, DR and /or Pal elements

1) Core

Nuclear receptor	Core
1A1 TRα	○
1B2 RARβ	○
1H3 LXRα	○
2C1 TR2	○
1D2 Rev-erbAβ	
1I1 VDR	
2A3 HNF4γ	
2B3 RXRγ	
2E1 TLX	
2F2 COUP-TFII	
2F6 EAR2	
4A1 NGFI-Bα	

2) DR

Nuclear receptor	DR 1	DR 2	DR 3	DR 4	DR 5
1B2 RARβ	○	○	○	○	○
2C1 TR2	○	○	○	○	○
2F2 COUP-TFII	○	○	○	○	○
2F6 EAR2	○	○	○	○	○
2A3 HNF4γ	○	○	○	○	○
1A1 TRα		○	○	○	○
1H3 LXRα		○	○	○	○
2B3 RXRγ	○	○	○		○
1D2 Rev-erbAβ		◉			
1I1 VDR			○		○
2E1 TLX					
4A1 NGFI-Bα					◉

3) Pal

Nuclear receptor	Pal0	Pal1	Pal2	Pal3	Pal4	Pal5
1H3 LXRα	○	○				○
2F2 COUP-TFII	○	○				
1D2 Rev-erbAβ	◉	◉		◉	◉	
2C1 TR2	○	○		○		○
1I1 VDR	○		○	○		○
1B2 RARβ	○		○	○		○
1A1 TRα	○			○		○
2A3 HNF4γ		○				○
2E1 TLX		○				○
2B3 RXRγ	○		○			○
2F6 EAR2	○	○	○	○		○
4A1NGFI-Bα	◉					

Fig. 4. Biochemical classification of human NHRs based on NHR–HRE binding specificities. Out of 34 synthesized NHRs, 24 bound to various DNA test elements. Thirty-four NHRs were divided into four groups on the basis on their binding specificities: (A) NHRs bound to all of the tested DNA elements with AGGTCA sequence (group A), (B) NHRs bound to two or more Core, DR and/or Pal DNA elements (group B), (C) NHRs bound specifically to only one type of DNA element (group C), and (D) NHRs not bound to any one of the tested DNA elements (group D). A positive NHR–HRE interaction is indicated with a colored circle (filled). Blank boxes in group D indicate that the NHRs listed did not interact with the Core, DR or Pal DNA element. NHRs having same or very similar DNA-binding activities are boxed in bold lines.

on the wheat germ extract cell-free expression system and the automated FCS technique offers a favorable methodology for the functional analysis of DNA–protein interactions. We also believe that the novel biochemical classification method described in this study might help in obtaining knowledge important for elucidating the NHR mediated-transcriptional network.

Further discussion is included in the supplementary data.

Acknowledgement: This work was partially supported by the Special Coordination Funds for Promoting Science and Technology by the Ministry of Education, Culture, Sports, Science and Technology, Japan (T.S. and Y.E.).

Appendix A. Supplementary data

Supplementary data associated with this article can be found, in the online version, at doi:10.1016/j.febslet.2008.07.003.

References

[1] Aranda, A. and Pascual, A. (2001) Nuclear hormone receptors gene expression. Physiol. Rev. 81, 1269–1304.
[2] Khorasanizadeh, S. and Rastinejad, F. (2001) Nuclear–receptor interactions on DNA-response elements. Trends Biochem. Sci. 26, 384–390.
[3] Ehrenberg, M., Cronvall, E. and Rigler, R. (1971) Fluorescence of proteins interacting with nucleic acids Correction for light absorption. FEBS Lett. 18, 199–203.
[4] Wolcke, J., Reimann, M., Klumpp, M., Göhler, T., Kim, E. and Deppert, W. (2003) Analysis of p53 "latency" and "activation" by fluorescence correlation spectroscopy Evidence for different modes of high affinity DNA binding. J. Biol. Chem. 278, 32587–32595.
[5] Kobayashi, T., Okamoto, N., Sawasaki, T. and Endo, Y. (2004) Detection of protein–DNA interactions in crude cellular extracts by fluorescence correlation spectroscopy. Anal. Biochem. 332, 58–66.
[6] Sawasaki, T., Ogasawara, T., Morishita, R. and Endo, Y. (2002) A cell-free protein synthesis system for high-throughput proteomics. Proc. Natl. Acad. Sci. USA 99, 14652–14657.
[7] Sawasaki, T., Hasegawa, Y., Tsuchimochi, M., Kamura, N., Ogasawara, T., Kuroita, T. and Endo, Y. (2002) A bilayer cell-free protein synthesis system for high-throughput screening of gene products. FEBS Lett. 514, 102–105.
[8] Mader, S., Leroy, P., Chen, J.Y. and Chambon, P. (1993) Multiple parameters control the selectivity of nuclear receptors for their response elements selectivity and promiscuity in response element recognition by retinoic acid receptors and retinoid X receptors. J. Biol. Chem. 268, 591–600.
[9] Carter, M.E., Gulick, T., Moore, D.D. and Kelly, D.P. (1994) A pleiotropic element in the medium-chain acyl coenzyme A dehydrogenase gene promoter mediates transcriptional regulation by multiple nuclear receptor transcription factors and defines novel receptor-DNA binding motifs. Mol. Cell. Biol. 14, 4360–4372.
[10] Maehara, K., Hida, T., Abe, Y., Koga, A., Ota, K. and Kutoh, E. (2003) Functional interference between estrogen-related receptor alpha and peroxisome proliferator-activated receptor alpha/9-cis-retinoic acid receptor alpha heterodimer complex in the nuclear receptor response element-1 of the medium chain acyl-coenzyme A dehydrogenase gene. J. Mol. Endocrinol. 31, 47–60.
[11] Okuno, M., Arimoto, E., Ikenobu, Y., Nishihara, T. and Imagawa, M. (2001) Dual DNA-binding specificity of peroxisome proliferator-activated receptor gamma controlled by heterodimer formation with retinoid X receptor alpha. Biochem. J. 353, 193–198.
[12] Retnakaran, R., Flock, G. and Giguère, V. (1994) Identification of RVR, a novel orphan nuclear receptor that acts as a negative transcriptional regulator. Mol. Endocrinol. 8, 1234–1244.
[13] Mader, S., Chen, J.Y., Chen, Z., White, J., Chambon, P. and Gronemeyer, H. (1993) The patterns of binding of RAR, RXR and TR homo- and heterodimers to direct repeats are dictated by the binding specificites of the DNA binding domains. EMBO J. 12, 5029–5041.
[14] Yen, P.M., Liu, Y., Sugawara, A. and Chin, W.W. (1996) Vitamin D receptors repress basal transcription and exert dominant negative activity on triiodothyronine-mediated transcriptional activity. J. Biol. Chem. 271, 10910–10916.
[15] Kliewer, S.A., Arimoto, E., Ikenobu, Y., Nishihara, T. and Imagawa, M. (1992) Convergence of 9-cis retinoic acid and peroxisome proliferator signalling pathways through heterodimer formation of their receptors. Nature 358, 771–774.

Biochemical and Biophysical Research Communications 370 (2008) 561–565

Contents lists available at ScienceDirect

Biochemical and Biophysical Research Communications

journal homepage: www.elsevier.com/locate/ybbrc

RIP and RALyase cleave the sarcin/ricin domain, a critical domain for ribosome function, during senescence of wheat coleoptiles

Tatsuya Sawasaki [a,c,*], Masahiro Nishihara [b], Yaeta Endo [a,c,*]

[a] Cell-free Science and Technology Research Center, The Venture Business Laboratory, Ehime University, 3 Bunkyo-cho, Matsuyama, Ehime 790-8577, Japan
[b] Iwate Biotechnology Research Center, 22-174-4 Narita, Kitakami, Iwate 024-0003, Japan
[c] RIKEN Genomic Sciences Center, 1-7-22 Suehiro-cho, Tsurumi, Yokohama 230-0045, Japan

ARTICLE INFO

Article history:
Received 20 March 2008
Available online 3 April 2008

Keywords:
Ribosome-inactivating protein
RNA apurinic site-specific lyase
Plant senescence
Sarcin/ricin domain
Programmed cell death
Wheat coleoptiles

ABSTRACT

Type-1 ribosome-inactivating protein (RIP), which is found in many plants, catalyzes depurination of a specific adenine in the sarcin/ricin domain (SRD) of the large rRNA causing loss of ribosomal activity. Previously, we found a RNA apurinic site-specific lyase (RALyase) that catalytically cleaved the phosphodiester bond at the RIP-dependent depurination site by β-elimination reaction. Here we show that both the RIP activity and RIP–RALyase-mediated cleavage of SRD in the cytoplasmic ribosome were induced at the late stage of senescence of wheat coleoptiles. Following this process, tissue death was observed. Furthermore, transgenic tobacco plants expressing glucocorticoid-induced RIP developed senescence-like phenotype. Our results suggest that ribosome inactivation due to the cleavage of SRD by the inducible RIP and constitutively expressed RALyase may be a unique plant system that mediates programmed cell death at the late senescent stage.

Plant senescence is a key developmental event because transport of nutrients, such as carbon and nitrogen, take place from the senescing leaves to the seeds for storage [1], and is thought to accompany programmed cell death [2]. Accordingly, many nutrient metabolism-related genes have been found to be expressed during the senescence stage [3]. However, the mechanism of the programmed cell death in senescence still remains elusive.

RIPs are classified into two broad groups: type-1 is a single-chain polypeptide and type-2 is a two-chain polypeptide, such as found in *Escherichia coli* O-157 vero toxin and ricin [4,5]. Recently, Stripe [6] proposed a third type (type-3) of RIP, which contained a polypeptide with unknown activity. The molecular basis of the RIP-mediated inactivation of ribosome involves hydrolysis of the *N*-glycosidic bond between the base and the ribose at position A4324 in the 28S rRNA of rat (reviewed in [7]). The hydrolysis site is embedded in a purine-rich single-stranded segment of 14 nucleotides and is nearly universal. This conserved sequence is called sarcin/ricin domain (SRD). Although over-expression of the type-2 RIP is known to kill animal cells [7], it is not known whether the type-1 RIP, found in many plant species [8], kills the host cells. We have previously reported that by removing the translational factors, including RIP, we were able to prepare a highly efficient and robust cell-free protein synthesis system from the wheat embryos [9,10], and demonstrated that this system was active for more than 14 days with the regular supply of substrates. Thus, it seems that the endogenous translational machinery is very robust.

RNA apurinic site-specific lyase (RALyase), found in the wheat germ extract [11] and rice plant [12], cleaves the phosphodiester bond at the RIP-dependent depurination site by a catalytic β-elimination reaction [11]. Thus, both RIP and RALyase cleave the SRD in the large rRNA. We have previously reported that the RIP–RALyase treatment inhibited the protein synthesis activity of the ribosome more strongly than the RIP treatment alone, which depurinated the rRNA but did not cleave the ribosome [13]. In mammalian cells, the RIP-induced damage to the 28S rRNA was shown to activate a novel kinase pathway known as ribotoxic stress response [14]. This ribotoxic stress response, which acts through the RNA-*N*-glycosidase, activates the cascades of the SAPK/JNK and p38-MAPK signaling pathways, and subsequently induces apoptosis [15]. These experimental evidences led us to hypothesize that in plants too RIP and/or RALyase could terminate the ribosomal activity when programmed cell death occurs in processes like plant senescence. In order to test our hypothesis, we investigated senescence in wheat coleoptiles and also in inducible RIP-expressing transgenic plants.

* Corresponding authors. Address: Cell-free Science and Technology Research Center, The Venture Business Laboratory, Ehime University, 3 Bunkyo-cho, Matsuyama, Ehime 790-8577, Japan. Fax: +81 89 9279941.
E-mail addresses: sawasaki@eng.ehime-u.ac.jp (T. Sawasaki), yendo@eng.ehime-u.ac.jp (Y. Endo).

0006-291X/$ - see front matter © 2008 Elsevier Inc. All rights reserved.
doi:10.1016/j.bbrc.2008.03.124